Title: On the energetic and structural retrofit of existing RC buildings through precast concrete panels: proposal of a new technology and explorative performance simulation

Authors: Silvia Martiradonna[1], Sergio Ruggieri[2*], Fabio Fatiguso[3], Giuseppina Uva[4], Ignacio Lombillo[5]

[1]Research fellow, Department of Civil, Environmental, Land, Building Engineering and Chemistry, DICATECH, Polytechnic University of Bari, Via Orabona, 4 – 70126, Italy, E-mail: silvia.martiradonna@poliba.it

[2]Assistant Professor, Department of Civil, Environmental, Land, Building Engineering and Chemistry, DICATECH, Polytechnic University of Bari, Via Orabona, 4 – 70126, Italy, E-mail: sergio.ruggieri@poliba.it

[3]Full Professor, Department of Civil, Environmental, Land, Building Engineering and Chemistry, DICATECH, Polytechnic University of Bari, Via Orabona, 4 – 70126, Italy, E-mail: fabio.fatiguso@poliba.it

[4]Full Professor, Department of Civil, Environmental, Land, Building Engineering and Chemistry, DICATECH, Polytechnic University of Bari, Via Orabona, 4 – 70126, Italy, E-mail: giuseppina.uva@poliba.it

[5]Associate Professor, Civil Engineering School, Structural Engineering & Mechanics Department, University of Cantabria, Avda. Los Castros s/n. 39005, Santander, Cantabria, Spain, E-mail: ignacio.lombillo@unican.es

*Corresponding author: Sergio Ruggieri, e-mail: sergio.ruggieri@poliba.it

Abstract: The paper presents the proposal of a retrofit system for reinforced concrete (RC) existing buildings consisting in the use of precast concrete panels designed for improving both structural and energetic performances. In particular, the proposed system is conceived, on one hand, for improving the energetic efficiency by ensuring high-performance thermal insulation and, on the other hand, for improving the capacity of structural elements under gravity and seismic loads. Firstly, the paper presents a detailed description of the proposed technology, which has been tested and assessed on a real-scale prototype. After, the efficiency of the technique has been explored by means of numerical simulations for both energetic and structural performances. Although no experimental tests are available, the response of numerical simulations and analyses on a real building case returns interesting insights, highlighting the main pros and cons of the proposal and providing a possible retrofit solution for buildings that do not meet the current European code requirements.

Keywords: Energetic Improvement; Structural Improvement; Precast Concrete Panels; Existing Buildings; Retrofit Systems.

1. Introduction

In the Mediterranean area more than 35% of the existing building stock is over 50 years old, evidence that emphasizes the high risk to suffer significant consequences due to the inefficiency in terms of structural and energy performances. In particular, reinforced concrete (RC) buildings constructed in the second post World-War present inadequate attributes from different points of view, such as old constructive technologies, absence of seismic details, structural and non-structural materials suffering decay, evidences that increase both structural and energetic vulnerabilities. Hazardous events as climate changes and earthquakes have led to the definition of new European policies for a global safer sustainable development that from one hand, aim to reduce greenhouse gas emissions and improve energy efficiency of the existing building stock and, from the other hand, aim to mitigate the risks related to the structural vulnerability.

From the structural and seismic vulnerability point of view, the effects of the recent earthquakes on the existing building stock, especially in the Mediterranean area, are in plain sight of everyone. In Italy, throughout the latest 50 years, about 10 medium-high earthquakes occurs, which raised the awareness of public institutions and the scientific community to collect data (Dolce et al., 2019) and to develop and promote seismic risk mitigation programs (e.g., Del Gaudio et al., 2020). To this, we add that more than the 70% of the existing building stock was built before the release of the first seismic building code, in the 1974 (ISTAT, 2011), and several seismic vulnerability sources could be denoted, e.g., poor quality of structural materials, low steel reinforcement in the beam-column joints and poor transverse reinforcement in the structural elements. From the energetic point of view, it is worth nothing that only about 1% of the European building stock has been renovated (European Commission, 2014), which is an alarming datum in this research field, considering that, as reported in (European Commission, 2019), the energy consumption shall be reduced at least of 32.5% up to 2030, by means of energy efficiency improvements. Under European directives, the National long-term strategies to support the building improvement and safety, involve the refurbishment of the elements belonging to the building envelope that have a significant impact in terms of performance. In this framework, besides to reduce risks due to earthquake, as one of the main hazardous sources of economic losses and fatalities, also energetic risks can be considered for developing better risk reduction strategies. As a matter of fact, from the energetic point of view, disregarding the seismic retrofit could not lead to a complete risk reduction, because seismic losses induce energetic losses (Belleri and Marini, 2015).

In recent years, some researchers have investigated retrofit methodologies accounting for the coupling of seismic and energetic vulnerabilities, proposing different techniques through a unique intervention (Bournas, 2018; Fumo et al., 2018). Interesting solutions regard the use of a double-skin (Manfredi and Masi, 2018), the use of an exoskeleton (Marini et al., 2017; D'angola et al., 2019) and the use of new and innovative materials (Manfredi and Masi, 2018; Artino et al., 2019). In general, new policies are strongly necessary to figure out this issue (e.g., Pohoryles et al., 2020) and to this noble scope, a possible solution developed during the last twenty years, is the use of prefabricated modules. Several international research groups have investigated prefabricated solutions with the aim to improve the building performance, thanks to the advantages related to the building refurbishment (e.g., speed, quality certification, safety, standardization, performance control, times, costs optimization, occupant disturbance minimization, environmental impacts). However, the two application fields (structural and energetic) have always been treated separately due to the several and often different variables to consider in the design phase.

Therefore, the goal of this paper is proposing a technological system that, based on precast concrete (PC) modules integrating recycled materials, aims to improve the building thermal insulation and to increase the structural capacity of existing frame structures under seismic actions. Throughout the document, we report a detailed description of the constructive technology for making the new system made by PC panels to apply on existing RC buildings. The feasibility of the proposed technique has been assessed on a real-scale prototype, constituted by an infilled RC trilith. Despite the existence of a prototype, no experimental tests have been carried out, considering that we are currently in the infant stages of this project. Nevertheless, in order to explore the possible energetic and structural efficiency of the proposed system as retrofit solution, numerical simulations have been performed by analysing the improvements obtained on the realized prototype and on a real building case. Within the analyses, energetic and seismic performances have been treated separately, investigating the effectiveness of the same system under different points of views. The results of numerical simulations provided new insights and perspectives in the adoption of the proposed technique on existing RC buildings, highlighting the main pros and cons and reserving further investigations for real structural and energetic tests.

2. State of the art: energetic and seismic retrofit of RC buildings using prefabricated modules

2.1. Energetic advantages

In the latest years, some important factors, e.g., economic crisis and climate change, have considerably influenced the construction sector. The growing demand of existing building renovation encouraged the scientific community to develop new solutions dedicated to convert the existing buildings into nearly zero energy buildings, NZEB. From the analysis of the literature regarding to the strategies about the improvements in building energy performance, it emerged that the restoration of the building facades has become the new challenge. The goal is to overcome the problem related to the traditional retrofitting intervention in terms of aesthetic dignity, low performance (Borodiniecs et al., 2017), high construction times and costs (Miloni, Grischott and Zimmermann, 2011). Off-site prefabrication can be the innovative and advantageous response to these issues. With the use of prefabricated modules, conventional formworks are eliminated, and props are reduced, as well as the production of wastage and various other environmental hazards are greatly dropped (Seghezzi and Masera, 2015).

Even in the recommendation document on building renovation of the European Union, the use of prefabricated solutions is strongly suggested (European Commission, 2019), and the use of prefabricated modules for building renovation has often demonstrated an increment of building energy performance (SKIN project, 2016; Azcarate-Aguerre et al., 2017; Konstantinou et al., 2017). Other researchers investigated different prefabricated solutions devoted to improve the façade performance of RC buildings. Pittau et al. (2017) have applied an innovative sandwich panel as a second skin of an existing residential building in Italy, achieving a total reduction of the primary energy consumption for heating of 82%. Silva et al. (2013) presented an application on two size type of buildings of a panel containing recycled materials involved reducing the overall energy needs, taking as reference the Portuguese contest. Garay, Arregi and Elguezabal (2017) have investigated the performance of a prefabricated module composed by a polyisocyanurate insulating layer and a photo-catalytic concrete finish, applied to a Spanish residential building.

Among the problems associated with the retrofit through prefabricated modules, dimensional adaptability and anchoring systems have been the most studied. As existing buildings have their geometric and dimensional characteristics, the notion of standardisation is lacking. A prefabricated module that adapts to an existing building cannot fit to another. For this reason, the concept of custom prefabrication born. Several researchers employed the technique of 3D laser scanning on RC existing buildings in order to acquire correct data on dimensions and geometrical features for the module design process (Borodinecs et al., 2017; Dobelis, Kalinka and Borodinecs, 2017; Borodinecs et al., 2018;

Pihelo, Kalamees and Kuusk, 2017). Nevertheless, the design of the anchoring system is still a hard challenge to face due to the materials compatibility, the fixing technology, the air tightness of the system and the thermal bridges that might occur along the edges of the panels. Silva et al. (2013) investigated a prefabricated retrofit module equipped with two steel U-profiles placed on each side of the modules and with a set of pins and holes to fit into a metal support structure already fixed to the existing wall. From the analysis of the thermal bridges, they observed that a significant heat flux occurred on the coupling area between the modules. Thus, they proposed some corrective measures on the distribution of the layers that drastically reduced the thermal losses. Annex (2011) employed some metal flats with one slotted hole and one or more round holes to suspend the modules. In the end, the most difficult challenge is to standardize the production of prefabricated systems, which is still an open issue in this research topic.

2.2. Structural and seismic improvements

A significant portion of the existing building stock worldwide is made by infilled RC buildings. The observations of the damages due to recent seismic events occurred in the Mediterranean area have suggested several vulnerability sources, with the necessity to investigate the role of all structural and non-structural elements in the seismic response of existing buildings. Most of the seismic collapses are due to failures of the masonry panels, which interact with the structural skeleton under horizontal actions and cause high economic and human losses. Masonry infills can induce some benefits in existing RC buildings, by increasing stiffness and strength and reducing the horizontal displacements caused by seismic actions (Negro and Colombo, 1997) but, on the other hand, infill panels provoke the increment of seismic demand on the surrounding frame, with consequent premature local collapses, induced also in the structural elements (Dolšek and Fajfar, 2001).

The scientific literature proposes extensive studies about linear and nonlinear behaviour of infilled RC frames subjected to seismic actions, among which numerical and experimental results (see Furtado and De Risi, 2020 and references therein). Two main failure categories are usually identified: in-plane (IP) and out-of-plane (OOP) mechanisms. Regarding the IP behaviour, the possible collapse mechanisms of masonry panels can be subdivided in shear, bending and compression failures, while for the RC frames, bending, axial, shear and beam-column joints failures are possible. A detailed overview is reported in Asteris et al. (2011) and El-Dakhakhni, Elgaaly and Hamid (2003), and the possible failure mechanisms are shown and listed in Figure 1. Concerning to OOP behaviour, the possible failures are due to different reasons, i.e., the presence or not of any kind of connections between the masonry and the surrounding RC frame, the panel support type and width, the presence of single or double leaf. In addition, of high importance are the other boundary conditions, as well as the panel slenderness (height/thickness) or the features of the upper bed joint. The possible failure path occurring for OOP actions can be observed as proposed by Pasca and Liberatore (2015), however, OOP failures could be schematized by defining kinematic mechanisms due to the occurrence of one or more yield-lines, as shown and listed in Figure 2. The interaction between IP and OOP behaviours can be also studied (Ricci, Di Domenico and Verderame, 2018; Di Domenico, Ricci and Verderame, 2019).

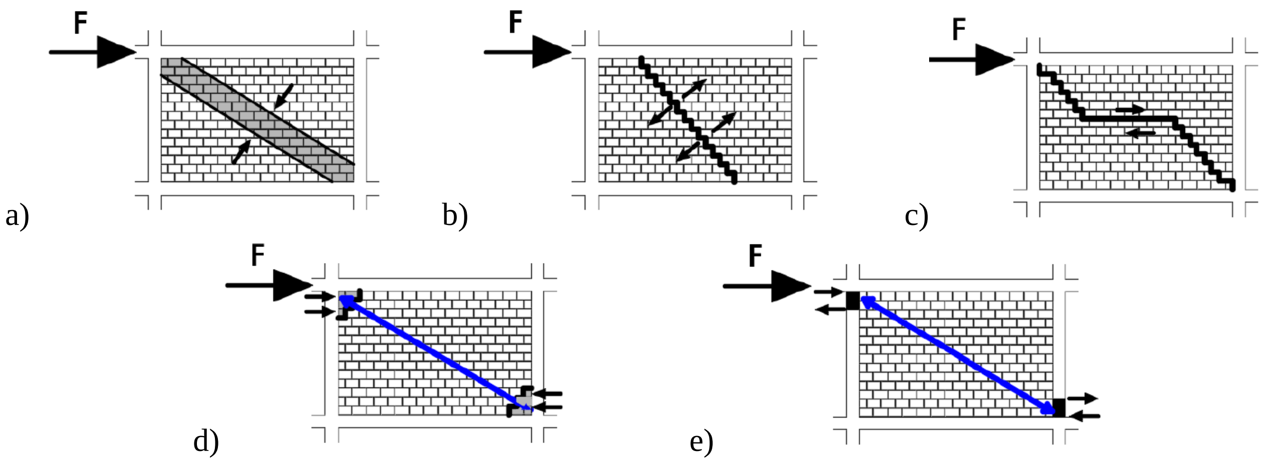

Figure 1 - Possible failure mechanisms of infilled frames under IP seismic actions (F): a) diagonal compression failure; b) diagonal cracking failure; c) sliding shear failure; d) corner crushing failure; e) frame failure crushing.

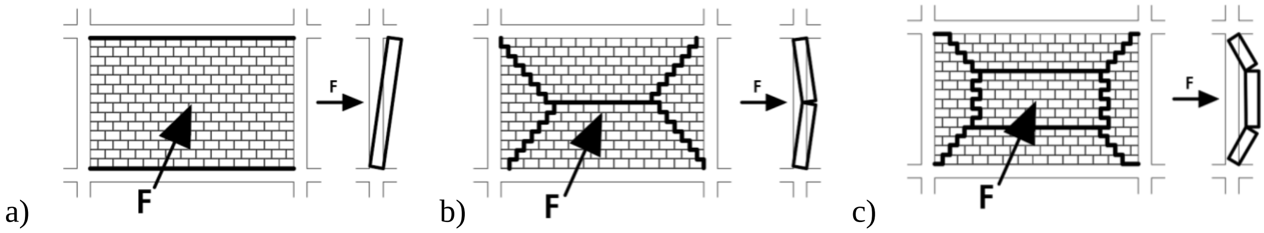

Figure 2 - Possible failure mechanisms of infilled frames under OOP seismic actions (F): a) rigid overturning of the masonry without arch effect; b) rigid overturning of the masonry with arch effect with one yield-lines; c) rigid overturning of the masonry with arch effect with two yield-lines.

Several retrofit methodologies have been proposed in the time, which are capable to improve both the IP and OOP behaviours, besides to provide benefits for the overall building response. Some strategies consist in the limitation of the masonry panel/surrounding frame interaction, by introducing a disconnection, e. g., using dissipative devices as sliding joints (Preti, Bettini and Plizzarri, 2012; Morandi, Milanesi and Magenes, 2018), vertical/horizontal collector beams (Basha and Kaushik, 2019), or isolating the structural frame from the masonry (Tsantilis and Triantafillou, 2018, Ju et al., 2012) by employing dissipative fuses in the perimeter of the infill (Lin et al., 2016). Other retrofit options consist in the application of layers of different materials (internal or external) to make solidarity between the masonry panel and the surrounding frame, e.g., textile-reinforced mortars (Koutas et al., 2014; Kaya, Tekeli and Anil, 2018; De Risi et al., 2020), fiber-reinforced polymers (Corte, Fiorinho and Mazzolani, 2008) and cementitious composites (Kyriakides and Billington, 2014; Valluzzi et al., 2014, Porco et al., 2018).

An additional retrofit technique that can be considered in the strengthening of infilled frame is the use of PC panels, applied internally/externally to the infill frame. Some application of this practice, with related experimental campaigns, are provided by literature. Baran et al. conducted experimental investigations on three one-third scale specimens to reproduce Turkish RC infilled frames and they applied internal PC panels for the entire surface of the masonry panels, 2 cm thick, by using plaster and epoxy mortar (Baran and Tankut, 2011; Baran et al., 2011). Akin and Sezer (2016) investigated six 2-storeys specimens by applying internal high-strength PC panels on the panel surface, made by different unit configurations. Ha et al. (2018) studied L-type PC panels considering the presence of openings. The results of experimental tests on six specimens suggested that the adopted method was adapt for low-rise buildings having openings and it ensured increment of lateral strength, stiffness and energy dissipation capacity. Choi et al. (2018, 2020) proposed to externally anchor PC panels, applied on the columns and beams using pretention bolts. Four specimens were investigated and the results of quasi-static loadings suggested reduced damages in the structural elements, with an increment of the lateral strength and stiffness. In analogy with this last methodology, our proposal consists in the application of external PC panels to existing infill RC frames buildings, with the additional task of increasing the energetic capacity of the existing buildings.

3. Combining energetic and seismic retrofit: proposal of the Intelligent Precast Concrete Panel System

The proposed system, named Intelligent Precast Concrete System (IPCS), is a new technology accounting for the energetic/seismic retrofit of existing RC buildings. The technology is based on the use of new PC panels fixed on the outer side of the existing façade by means of steel mullions and hooks which guarantee the vertical position thanks to the function of internal retaining excluding the use of external props during the installation. To complete and stiffen the entire wall, the system provides a completion casting in lightweight concrete into the resulting cavity between the new precast wall and the existing one, as an additional RC filling layer. The entire system is connected to the existing RC frame by means of post-installed rebars fixed by chemical epoxy resin injections. The system is designed to be equipped with its own continuous foundation along the portions of the facade on which it is applied, thus, the technology does not burden the existing structure, on the contrary, it stiffens and collaborates with it so that it can withstand seismic actions. Regarding to the new foundation, its main role is to face the increment of stresses given by the new system (e.g., axial, bending and shear forces) and, in addition, it allows to improve the structural performance of the overall system composed by the existing building and the retrofit panel under static and seismic actions. To avoid the expulsion of the masonry panels towards the inside of the building because of the hydrostatic pressure due to the completion jet of the lightened concrete, the building wall is previously protected by panels of recycled Expanded Polystyrene Sintered (EPS) which, in addition, improve the energy performance of the whole system. The insulating blocks are spaced 5 cm from the frame, leaving free the joints between beams, columns and wall to strengthen them with the completion concrete and generate a box effect of the building (Martiradonna, 2021). The model of the technology is shown in Figure 3. Still, the term "intelligent" is adopted in the name because it can be predisposed to be easily equipped with monitoring devices to control the performance trend of the building façade over time. They are accommodated into steel mullions, suitable shaped to permit their easily installation and provide the possibility to maintain and remove them at any time, also during the installation phases, after anchoring the mullions at the frame structure.

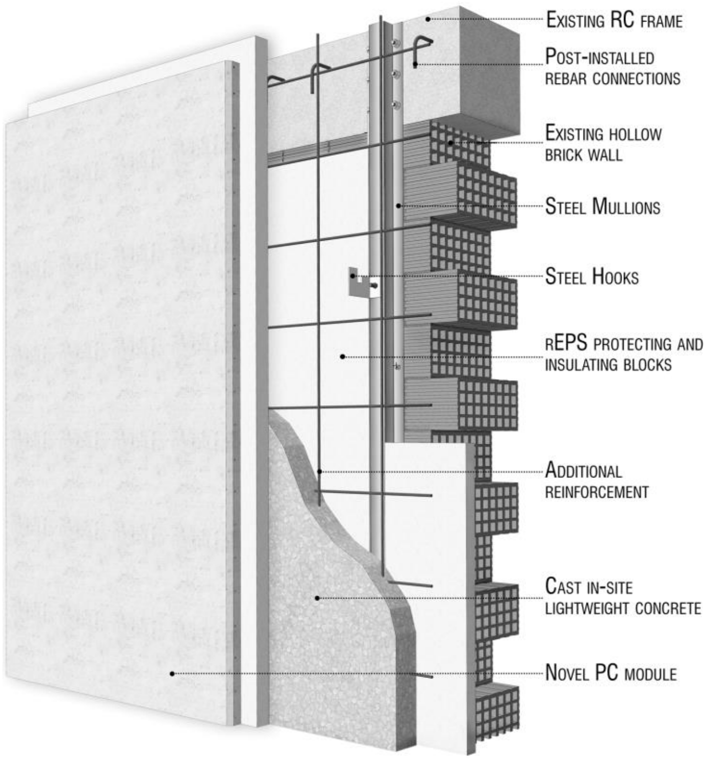

Figure 3 – Draft of the proposed retrofitting system technology.

The main element that characterizes the system is a PC panel consisting in two layers: the external reinforced concrete slab and the internal insulation sheet in lightweight mortar (LWM) and recycled EPS blocks. This internal insulating coat is disposed on the inner slab surface in a staggered way to create the male-female configuration of junctions with the aim to prevent the generation of possible thermal bridges. The panel reinforcement is designed to anchor the module to the existing façade and consists in steel lattices disposed along the panel width and steel rebar arranged in both directions and embedded into the slab thickness. The dimensions of the modules and the trusses arrangement may vary for aesthetic needs and adaptation to the existing building, within the specified limits. However, the standard module is 1.2 m in width and 2 m in length (Martiradonna, 2021). Figure 4 highlights the arrangement of the panel components.

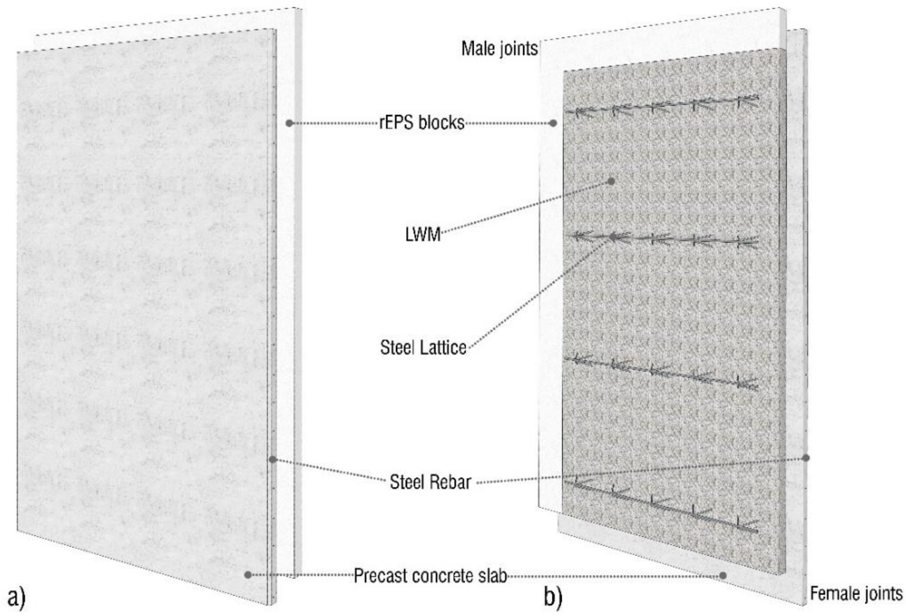

Figure 4 – The PC panel: a) external face; b) internal face.

The distinguishing elements of the system are the steel mullions and hooks used to connect the PC modules to the existing building façade. Thanks to accurately designed anchoring elements, used to fix them to the existing RC frame, they are fundamental for the system tightness during the mounting phase of PC modules, the cast-in-place concrete, and monitoring stage. The mullions and the hooks are in hot galvanised steel for structural use, e.g., type S235JR, classified according to European building code (Eurocode 3, 2004). In particular, the mullions have a hot rolled omega profile, suitably shaped for the monitoring sensors lodging in the core and for the anchoring positioning into the slots, dimensioned and spaced according to the anchoring determination. The hooks are designed to meet the steel latticework embedded in concrete slab and withstand the traction forces induced by the PC panels from the moment of the installation to the cast-in-place concrete.

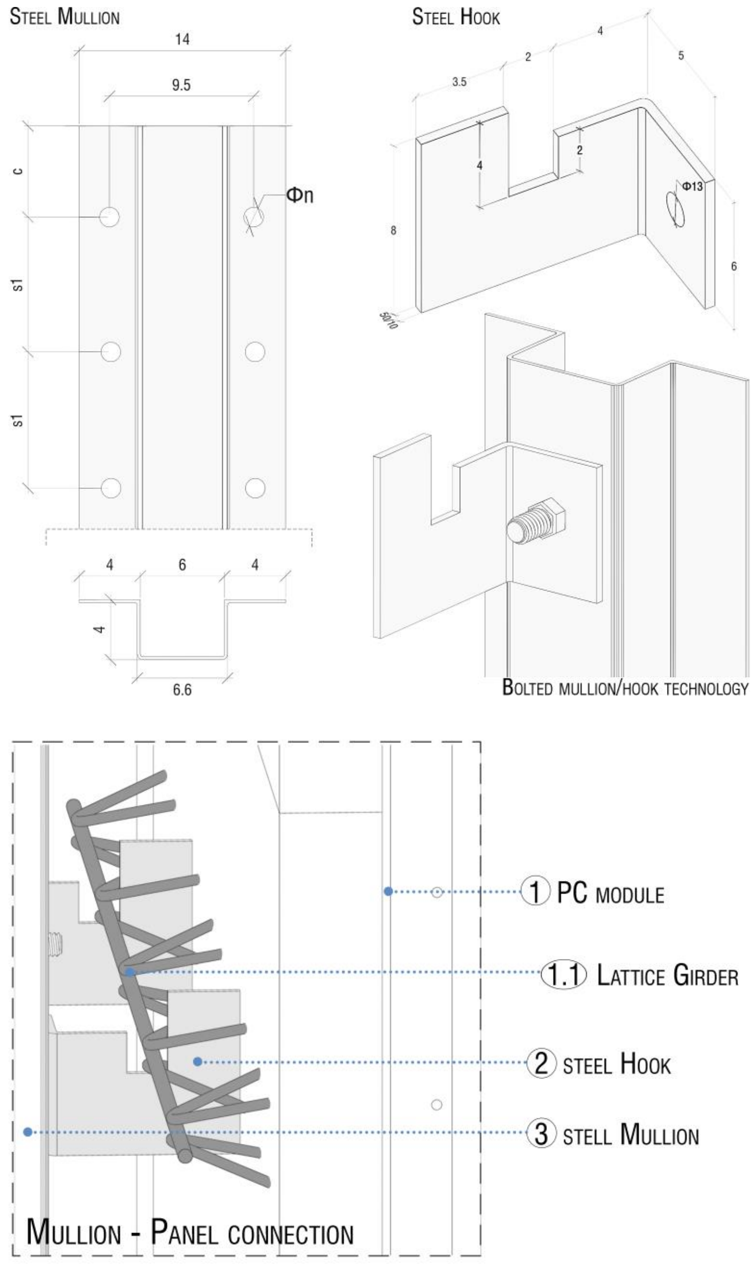

Figure 5 – Steel mullion, anchor and the bolted technology.

Their height determines the concrete layer thickness which should be defined in accordance with the results of the preliminary structural analyses aiming at understanding the building behaviour with the applied system. To assure a strength connection of the mullions to the existing RC beams, the chemical anchoring method is used. In Figure 5 is shown the mullion/hook technology and the panel anchoring to the hooks. As regard the connection between the existing RC frame rebars with the wall reinforcement, the post-installed rebar technology is employed. The bars are made by improved adhesion steel, e.g., type B450C for structural use, shaped as hooks complying with the Italian Building Code (2018) directive. It is assumed that they are installed into the existing RC frame to ensure the adequate iron cover, safely transmitting the forces to the concrete avoiding longitudinal cracking or spalling. They are connected to the steel reinforcement of the wall in cast in-site lightweight structural concrete (LWSC) identified as a weakly armed concrete wall as defined by the Italian legislation. In Figure 6, the concept of the system technology and anchoring is illustrated as well as the plant view of the proposal technology applied to an infilled RC frame is shown.

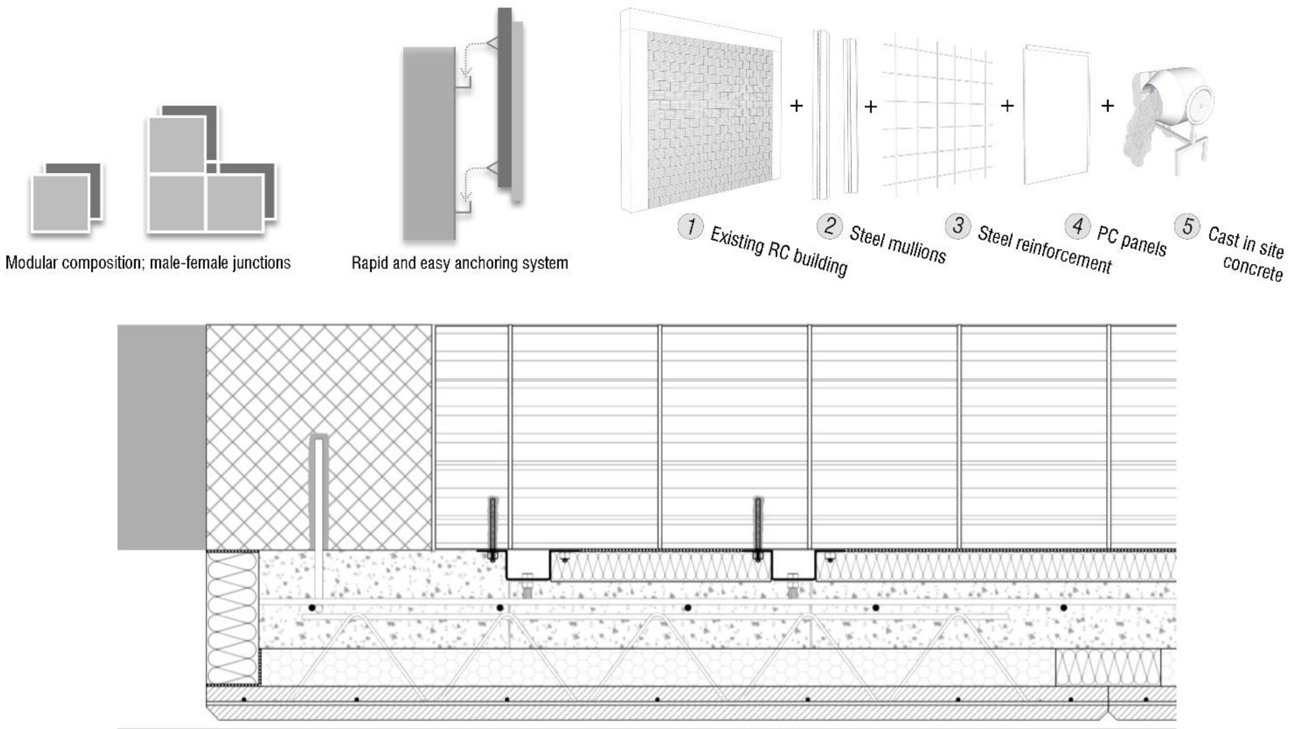

Figure 6 – Retrofit of the infill RC frame by means of IPCS: concept of technology and anchoring system and plant view.

4. Assessment of the IPCS technology on a real-scale prototype of infilled RC frame.

4.1. Input data for design and application of the IPCS

The design idea of the proposed technological system takes in account the compatibility of the novel building components with the existing materials and constructed methods. Its details make it easily adaptable to different building typologies, although the technical details, the element dimensioning, calculation, and the performance assessment should be carried out case by case in function of the geometry, materials and loads of the case study. The building typology considered to design and analyse the proposal technology is a multi-family house (MFH) of the second post World War (post-WW2), especially for their great deficiencies in terms of thermal and structural performance. Being the widespread typology in Italy and in many other countries, they are responsible of a great energy consumption and endanger the health of citizens. Moreover, they have a very simple shape, and their constructive and technical characteristics are approximately the same in the European countries with similar climate conditions. The external RC frame usually stays along the perimeter of the building to anchor and link the existing structure to the modules. The geographic area of study for the IPCS design is the South of Italy, in particular Bari district in Puglia Region as result of the deep climatic and seismic analysis of Italy. The considered input data for the design and application of the IPCS are summarized in Table 1, where DD or degree-days indicates the parameters that quantify the average thermal requirement necessary to maintain an indoor comfortable climate during the year in a specific location; PGA indicates the values of the peak ground acceleration on rigid soil; U-value is the value of the thermal transmittance of the building component. The average conditions of temperature (T°) and relative humidity (RH) to consider for carrying out the thermo-hygrometric studies are defined as follows:

- indoor conditions, corresponding to the ideal comfortable values, are T° 293.15 K and RH 52%.
- outdoor conditions are T° 281.55 K and RH 68%.

The climatic data are selected from Bari Karol Wojtyla weather station, Italy (WMO: 162700) by ASHRAE Climatic Design Conditions 2003/2013/2017. The mean values from the table of "Monthly Climatic Design Conditions in 2017" are considered, in particular looking data from

February, the coldest month of the year. Despite in the referred month lower peak values of T° and RH occur, the design criteria of the analyses are the mean values (Martiradonna, Fatiguso and Lombillo, 2020). Thanks to the definition of the boundary conditions to design the IPCS, singular explorative methodology of analysis about thermal and structural behaviour are proposed in the following sections.

Table 1 – Input data to design the proposed technological system

Input data	
Italian Region District	Bari, Puglia Region
Climate Zone	DD = 1185 limit U-value= 0.36 W/(m^{2}K)
Seismic Zone	0.05 < PGA ≤ 0.15
Building Typology	MFH
Façade Typology	Hollow brick wall Thickness 30 cm Post-WW2
U-Value	1.25 W/(m^{2}K)

4.2. Real-scale prototype realization

The definition of the geometric and physical characteristics as well as the interaction between the novel system and the existing structure has been assessed by employing a real-scale prototype. To this scope, a reduced infilled frame model, 3 m x 3 m, is considered (Figure 7), with the purpose of reproducing the coupled behaviour of existing building and the proposed system. Herein, it is useless to specify all the parameters characterizing the prototype, considering that the unique scope of the test was the technological assessment of the retrofit methodology. To this aim, Figure 8 reports all construction phases of the IPCS prototype, according to the description reported in Section 3: a) constitution of the panel with an industrial process; b) finished IPCS; c) infilled frame with application of one panel; d) lateral detail of the system; e) casting of lightening concrete layer; f) final result of the prototype. Once observed the outcome of the retrofit application with all the related construction phases, the exploration of the energetic and seismic is carried out by numerical models on the basis of several assumptions, properly specified for the two application fields. The methodology employed, from the model setting to the results reading, is based on the actual standards and the methods proposed in the scientific literature. The numerical and qualitative evaluations are carried out by means of finite element (FE) models, both for the thermal and structural evaluations. In the end, it is possible to show some photos about the construction phases and the applications of the IPCS on the real infilled frame prototype, as reported in Figure 8. In this latter are reported the details of the IPCS panel production, the application of the system to the infilled frame prototype and the result obtained according to the procedure reported in Section 3. Moreover, some detailed photographs of the IPCS panel anchoring are provided in Figure 9, in particular, the reinforced chemical injection of the steel mullions to the existing RC structure, the installation phase of the panel to the existing frame and the final aspect of the anchoring technology in lateral and upper view (correspondence with sketch at Figure 5).

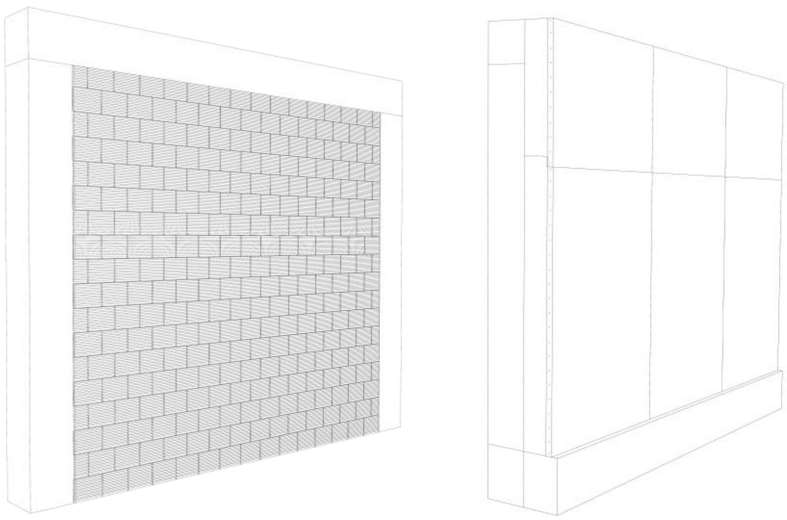

Figure 7 – Sketch of the real-scale prototype: existing RC and retrofitted frames.

Figure 8 – Construction phases and application of the IPCS prototype: a) constitution of the panel with an industrial process; b) finished IPCS; c) infilled frame with application of one panel; d) lateral detail of the system; e) casting of lightening concrete layer; f) final result of the prototype.

Looking at the realized IPCS prototype, some information about the costs of the proposed retrofit technique can be provided. In detail, expressing the unitary cost in €/m^2, the price of the system and its application has a cost of 200 €/m^2, calculated in accordance with the company partner of the project. This datum is important, especially if compared with the cost of other structural/seismic and energetic retrofit techniques, as individually considered. For the case at hand and for the Italian case, considering the price list of building works and interventions recently released by Abruzzi Region (2022) and the most practical techniques for energetic retrofit, the costs of the interventions go from 30 €/m^2 for thermal insulation of building roof, 60 €/m^2 for thermal insulation of building envelope, 100 €/m^2 for low emissivity windows and 150 €/m^2 for HVAC (heating, ventilation and air conditioning) system.

Figure 9 – Details of the construction phases and application of the IPCS prototype: a) reinforced chemical injection for steel mullion anchoring; b) reinforced chemical injection to connect the existing reinforcement with the new one; c) final aspect of the wall ready to receive the panel; d) IPCS installation; e) final aspect of the anchoring technology in lateral view; f) final aspect of the anchoring technology in upper view.

Analogously, considering the above price list and the most practical structural and seismic retrofit techniques, the costs of the interventions go from 120 €/m^2 for RC jacketing, 170 €/m^2 for the realization of RC walls, 250 €/m^2 for interventions using fiber reinforced polymer (FRP) materials and 470 €/m^2 for steel jacketing. Although the evident increment of weight (about 50 kN/m^3), the reported list of prices of retrofit interventions suggests how the proposed panel can be advantageous from the economic point of view with regard to other common techniques, especially considering that the proposed system combines energetic and seismic retrofit and, once again, the application of the system minimizes the interruption of the building use and the invasiveness of the intervention itself and, at the same time, reduces the number of working days and manpower employed.

4.3. Preliminary evaluation on the prototype thermal behaviour

The evaluation of the thermal behaviour of the selected façade typology is carried out under the stationary and dynamic climatic conditions in order to appraise the thermal resistance and inertia. In addition, the estimation of the resistance to vapour diffusion is performed in order to study the hygrometric behaviour wall, considering the steady-state procedure by EN ISO 13788 (2013). Starting from the definition of these parameters, the evaluation methodology can be specified. According to EN ISO 6946 (2018), the thermal resistance (R-value) in stationary conditions, is the capacity of the wall to resist to the heat flow. It is the mutual value of the coefficient of heat transmission between surfaces namely thermal transmittance (U-value), which represents the heat flow that goes through a unit thickness surface subjected to a temperature difference of a Kelvin degree (EN ISO 6946, 2018). It depends on the thermal conductivity coefficient (λ), which represents the capacity of a material to heat transferring. The Italian guidelines (DM 26/06/2015) fix the limit R-value of the existing building walls subjected to energy improvements to 2.77 m^2K/W that corresponds to a U-value of 0.36 W/m^2K (U_{max}). At lower U-values correspond a better thermal performance of the building component. The resistance to vapour diffusion is the capacity of the wall to impede the water vapour diffusion through its layers. It depends on the dimensionless coefficient of vapour diffusion resistivity (μ) which characterizes each material (EN ISO 6946, 2018). To evaluate the wall thermal capacity in dynamic conditions, i.e., at temperature variation, the thermal inertia has to be considered. According to EN ISO 13786 (2018), it is the capacity of a building component to mitigate the indoor temperature fluctuations due to the variation of thermal loads throughout the day, and to accumulate and release heat after several hours. To appreciate the wall thermal inertia in a simplified way, the principle dynamic parameters are considered: the periodic thermal transmittance (Y_{ie}) and the periodic internal thermal capacity (k_1). The first estimates the heat shift for 24 hours and it is defined as the ratio of the flow induced internally by a periodic sinusoidal variation of the external temperature to the variation itself. The second is the effective thermal accumulation capacity of the wall and it is the product between the specific wall heat and the surface thermal mass (m_s). High performance of the wall, thus a reduced energy requirement for summer cooling, is determined by a periodic thermal transmittance value lower than 0.10 W/m^{2}K (with a time shift coefficient, φ, greater than 12 hours and attenuation factor, f_d, lower than 0.15), and a high value of periodic internal thermal capacity (Perna et al., 2009). These parameters are calculated according to the methodology in in Ursini Casalena (2018). The Italian standard also establishes the limit values (indicates with *lim* subscript) of the dynamic parameters as: $Y_{ie,lim} < 0.10$ W/m^{2}K; $k_{1,lim} \geq 50$ kJ/m^{2}K; $m_{s,lim} > 230$ kg/m^3; $f_{d,lim} < 0.6$.

For the preliminary assessment of the steady-state thermo-hygrometric behaviour of the reduced wall considered for this study, four main portions are taken in account due to the variation of the stratigraphy:

a. Type a: 30 cm hollow brick + 5 cm rEPS block + 10 cm LWSC + 5 cm LWM + 4,5 cm Concrete slab (Table 2).
b. Type b: 30 cm hollow brick + 4 cm air + 0.3 cm steel mullion + 10 cm LWSC + 5 cm LWM + 4,5 cm Concrete slab (Table 3).
c. Type c: 30 cm RC (beam) + 15 cm LWSC + 5 cm LWM + 4,5 cm Concrete slab (Table 4).
d. Type d: 30 cm RC (beam) + 4 cm air + 0.3 cm steel mullion+ 10 cm LWSC + 5 cm LWM + 4,5 cm Concrete slab (Table 5).

Table 2 - Wall stratigraphy Type a

Wall Layer	d (mm)	ρ (daN/m^3)	λ (W/mK)	μ
Indoor heat transfer coefficient			7.70	
Hollow brick	300	1200	0.50	9.30
rEPS block	50	10	0.04	20
LWSC	100	1978	1.35	42.46
LWM	50	187.7	0.0587	6.50
Concrete slab	45	2400	2.00	47.85
Outdoor heat transfer coefficient			25.0	

Table 3 - Wall stratigraphy type b

Wall Layer	d (mm)	ρ (daN/m^3)	λ (W/mK)	μ
Indoor heat transfer coefficient			7.70	
Hollow brick	300	1200	0.50	9.30
Air	40	1.225	0.026	1
Steel mullion	3	7850	79	2×10^6
LWSC	100	1978	1.35	42.46
LWM	50	187.7	0.0587	6.50
Concrete slab	45	2400	2.00	47.85
Outdoor heat transfer coefficient			25.0	

Table 4 - Wall stratigraphy type c

Wall Layer	d (mm)	ρ (daN/m^3)	λ (W/mK)	μ
Indoor heat transfer coefficient			7.70	
RC (beam)	300	1200	0.50	9.30
LWSC	150	1978	1.35	42.46
LWM	50	187.7	0.0587	6.50
Concrete slab	45	2400	2.00	47.85
Outdoor heat transfer coefficient			25.0	

Hence, the thermal transmittance values of the four wall portions are computed in accordance with the procedure in (Garay, Arregi and Elguezabal, 2017; Martiradonna, 2021; EN ISO 6946, 2018), and compared with the limit value, U_{max}, established by Italian guidelines (DM 26/06/ 2015):

a. U_a = 0.31 W/m^{2}K < U_{max}.

b. U_b = 0.28 W/m^{2}K < U_{max}.

c. U_c = 0.77 W/m^{2}K > U_{max}.

d. $U_d = 0.36$ W/m^{2}K = U_{max}.

The overall U-value of the wall (U_w) is the weighted mean value of the four types (using d as weighting factor) and is equal to 0.4307 W/m^{2}K. It is clear that it does not comply with the standard due to the high values reached in type c and d. Although, thanks to the panel configuration (i.e., the horizontal direction of the steel latticework), it is possible to vary the distribution of the insulating materials in order to match the section of the beam the panel portion with the rEPS block, positioned within the spacing of the lattices. Type e and type f would be the new stratigraphy that replace type c and type d, respectively:

e. 30 cm RC (beam) + 12 cm LWSC + 8 cm rEPS block + 4,5 cm Concrete slab (Table 6);

f. 30 cm RC (beam) + 4 cm air + 0.3 cm steel mullion + 7 cm LWSC + 8 cm LWM + 4,5 cm Concrete slab (Table 7).

Table 5 - Wall stratigraphy type d

Wall Layer	d (mm)	ρ (daN/m^3)	λ (W/mK)	μ
Indoor heat transfer coefficient			7.70	
RC (beam)	300	1200	0.50	9.30
Air	40	1.225	0.026	1
Steel mullion	3	7850	79	2×10^6
LWSC	100	1978	1.35	42.46
LWM	50	187.7	0.0587	6.50
Concrete slab	45	2400	2.00	47.85
Outdoor heat transfer coefficient			25.0	

Table 6 - Wall stratigraphy type e

Wall Layer	d (mm)	ρ (daN/m^3)	λ (W/mK)	μ
Indoor heat transfer coefficient			7.70	
RC (beam)	300	1200	0.50	9.30
LWSC	120	1978	1.35	42.46
rEPS block	80	10	0.04	20
Concrete slab	45	2400	2.00	47.85
Outdoor heat transfer coefficient			25.0	

Table 7 - Wall stratigraphy type f

Wall Layer	d (mm)	ρ (daN/m^3)	λ (W/mK)	μ
Indoor heat transfer coefficient			7.70	
RC (beam)	300	1200	0.50	9.30
Air	40	1.225	0.026	1
Steel mullion	3	7850	79	2 x 10^6
LWSC	70	1978	1.35	42.46
rEPS block	80	10	0.04	20
Concrete slab	45	2400	2.00	47.85
Outdoor heat transfer coefficient			25.0	

The U_e-value and U_f-value are 0.35 W/m^{2}K and 0.25 W/m^{2}K, respectively. Therefore, the U_w-value, computed as previously done, is equal to 0.2977 W/m^{2}K, which complies with the standard. Considering the assumed climatic conditions (indoor: T°=293.15 K; RH=52%; outdoor: T°=281.55 K; RH=68%), the evaluation of the hygrometric behaviour of the wall starts from the calculation of the superficial temperature of each layer. The software COMSOL Multiphysics (COMSOL, 2018) is used to create the FE 3D model of the wall, calculate the temperature distribution in the specific sections and observe the heat flux development through the temperature iso-curves.

The visual survey of the 3D models and in particular the temperature variation scale, provides information about the thermal bridges' generation (Martiradonna, Fatiguso and Lombillo, 2020). Applying the procedure by EN ISO 13788 (2013), the Glaser's diagrams are drawn in order to understand the interstitial condensation hazard, in particular in the sections with the steel mullions. The interstitial condensation occurs if the saturation pressure curve intersects the vapour pressure one. The following Figures investigate (i) the temperature distribution, (ii) the related Glaser's diagrams, (iii) the thermal bridges for the sections type a (Figure 10), type b (Figure 11), type e (Figure 12) and type f (Figure 13). The section with the post-installed connection is analysed in Figure 14.

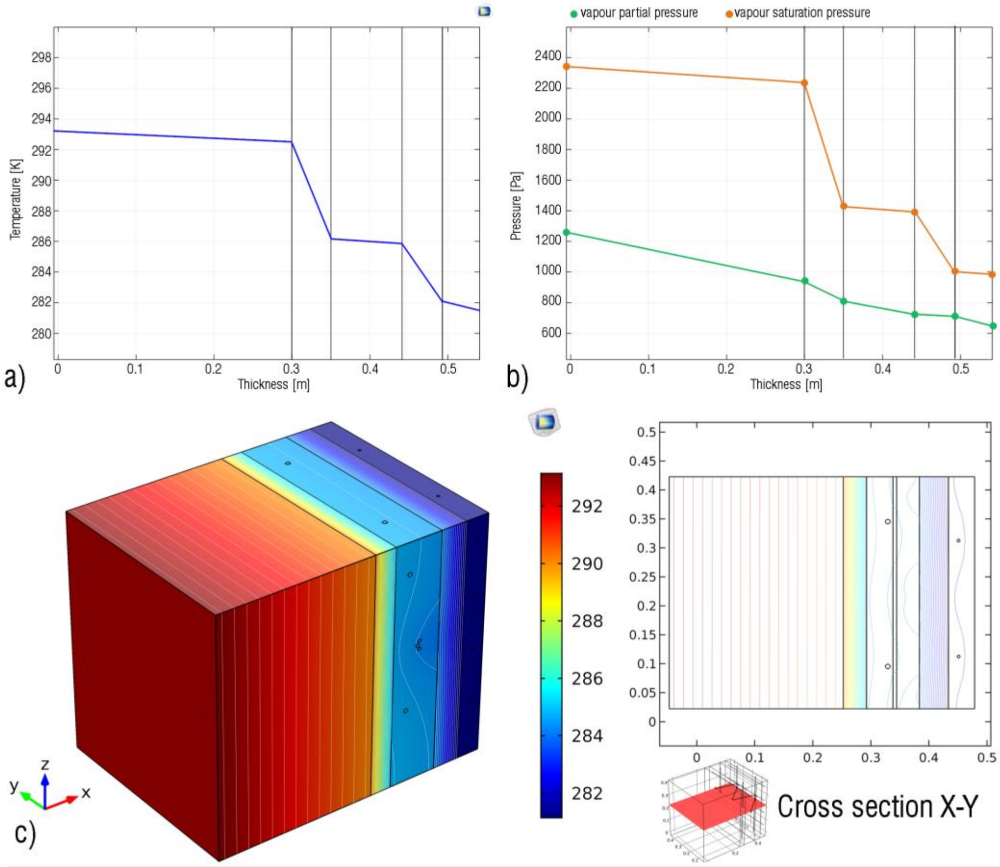

Figure 10 - Hygrometric behaviour and thermal bridges formation: wall portion type a.

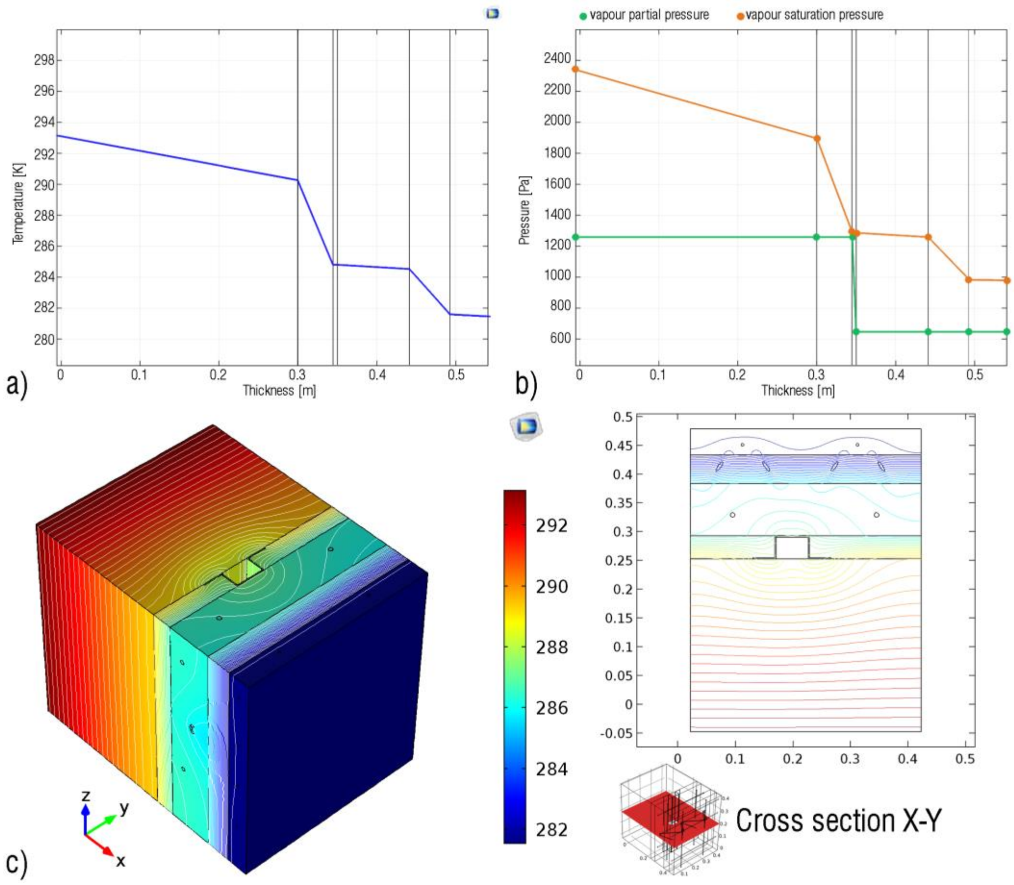

Figure 11 - Hygrometric behaviour and thermal bridges formation: wall portion type b.

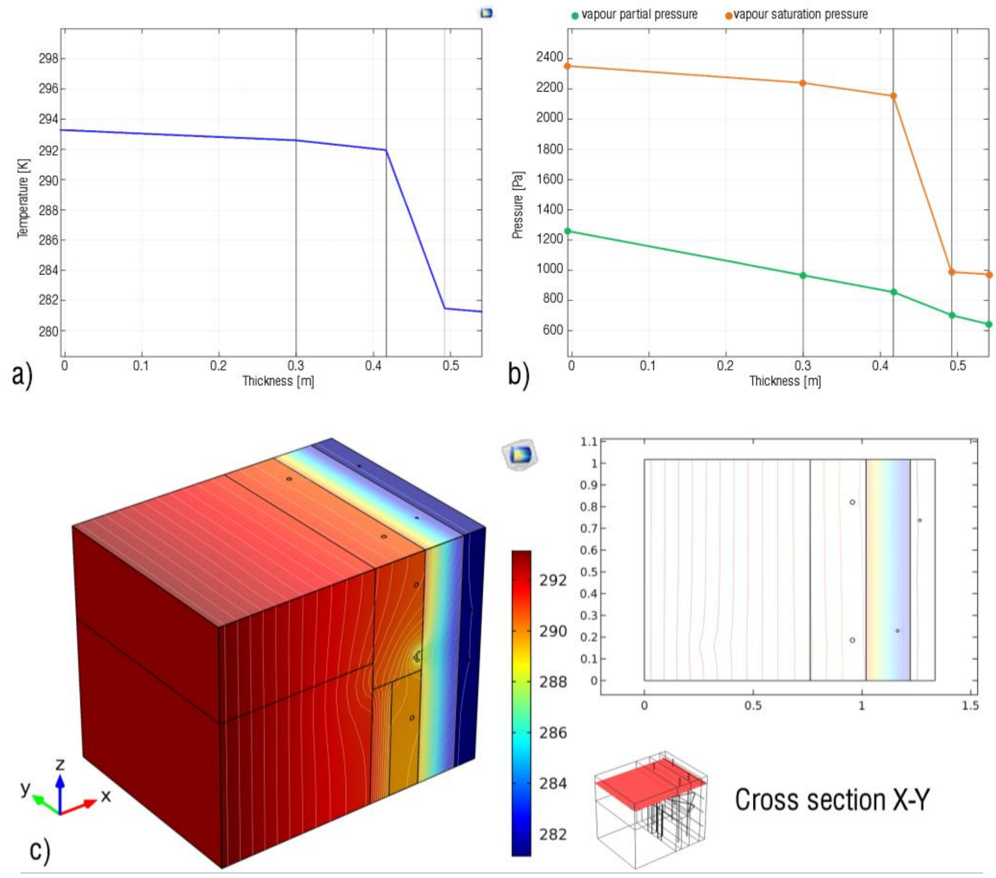

Figure 12 - Hygrometric behaviour and thermal bridges formation: wall portion type e.

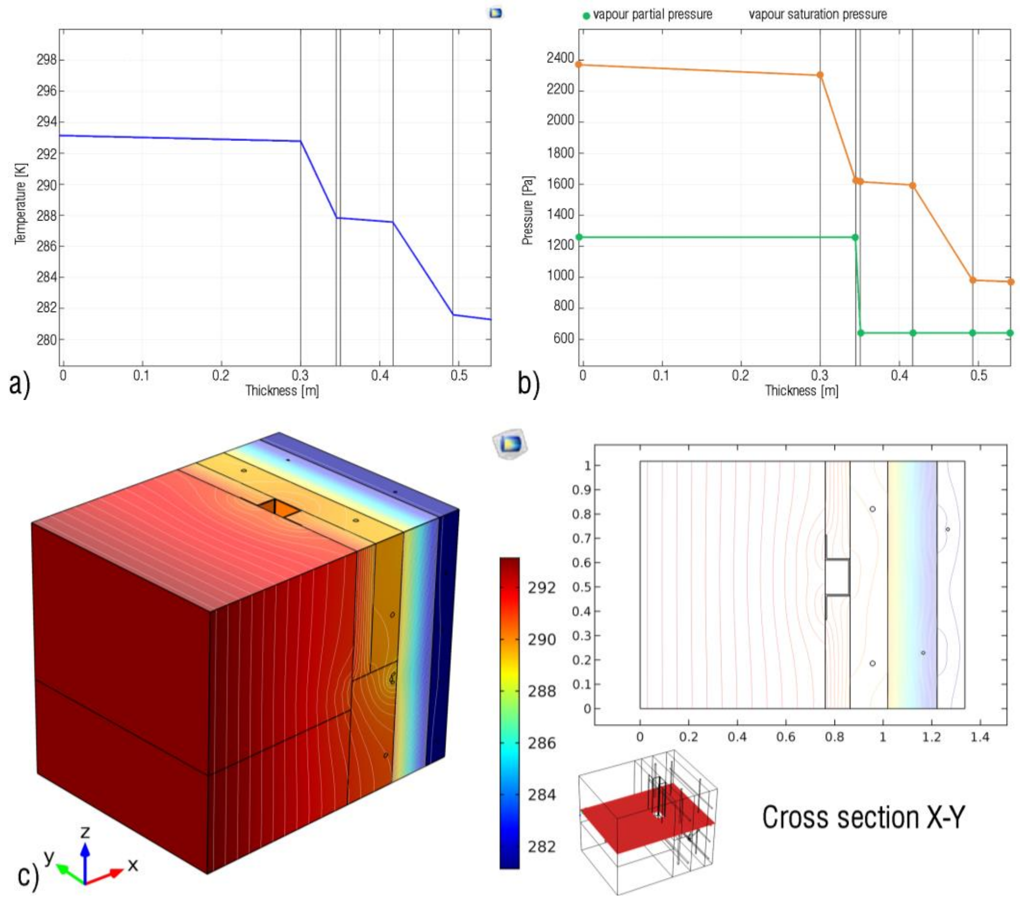

Figure 13 – Hygrometric behaviour and thermal bridges formation: wall portion type f.

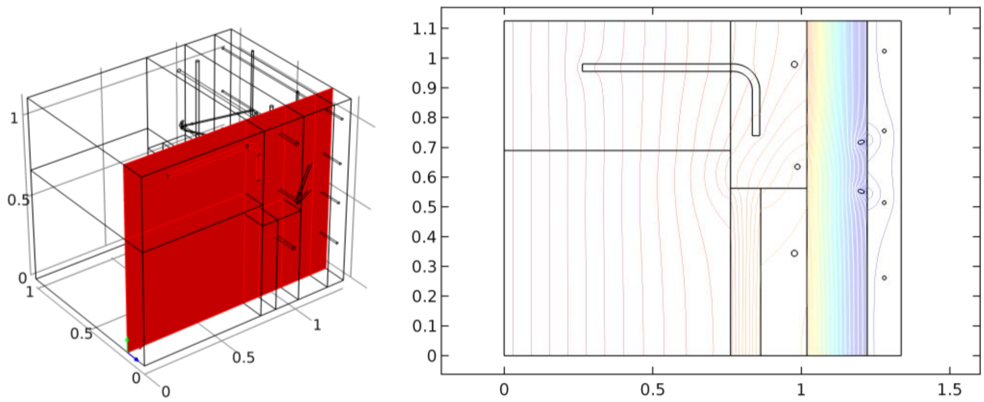

Figure 14 – Heat flux distribution in the section X-Z: post-installed connection.

Thanks to the distribution, thickness and properties of the layers, no condensation occurs in any section for the values of temperature and relative humidity considered. In the wall section type b, especially in correspondence of the steel mullion, the curves of vapour partial and saturation pressures peak due to the waterproof properties of the mullion that does not spread water vapour. However, for the mean conditions considered for the analysis, the curves do not intersect, thus, no condensation occurs. Nevertheless, it is not excluded that it generates condensation in more severe climatic situations. However, considering the results of the other sections and that iron is a good heat conductor, the temperature along the mullions would be the weighted average of all the temperatures of the individual sections. Therefore, the surface temperature value of the mullions on the resulting curve would have a higher value than the one of section type b. This would result in a deviation of the pressure curves, thus removing the risk of condensation. Certainly, further insights will be developed in the future, through the use of global behaviour assessment software as performed by Silva et al., (2013) and experimental tests. The 3D analysis of the temperature iso-curves shows that, despite the presence of steel elements in all sections, no thermal bridges occur. Thermal flux disturbances are observed near to the reinforcements; however, they do not affect the overall performance of the system. As regard to the evaluation of the thermal performance in dynamic-state, thus, the wall thermal inertia, the computation of the periodic thermal transmittance and the periodic internal thermal capacity is carried out thanks to the methodology proposed by Ursini Casalena

(2018), taking into account the resulting values of the time shift coefficient and attenuation factor. The results of the calculation are: Y_{ie} = 0.003 W/m^{2}K < $Y_{ie,lim}$; k_1 = 53.5 kJ/m^{2}K > $k_{1,lim}$; m_s = 714 kg/m^3 > $m_{s,lim}$; f_d = 0.01 < $f_{d,lim}$; φ = 21.3 h.

The values comply with the standard limit values. In particular, the time shift value φ is very high, meaning that the wall is able to retain and release the heat only after 21 hours of exposure to hot summer temperatures, keeping the indoor environment at temperatures lower than outside, thus, decreasing the energy requirement for cooling. Therefore, agreeing with the considerations by Perna et al. (2009), the system presents excellent performance in dynamic regime.

4.4. Preliminary evaluation on the prototype structural and seismic behaviour

Close to the energetic retrofit, the proposal has like important objective to give an opportunity of structural upgrading, able to minimize the interruption of the building use and the invasiveness of the interventions. Hence, it is immediately glaring that the nature of the proposed system leads to a substantial variation of the structural response of the original building, due to an increment of mass and stiffness. Especially in the presence of seismic actions, it is necessary to evaluate how the structural capacity is modified, in terms of both strength, stiffness and ductility. To this end, an exploratory analysis has been carried out, adopting a meso-modelling approach, as later described, which is sufficiently lean and manageable, especially considering that currently no experiments have been carried out for the mechanical characterization of materials and structural tests on prototypes, and therefore no specific reference data are available. This approach will be applied to a case study to globally test the effects on structural response. Of course, it must be stressed that the evaluations made on the effectiveness and limitations of the results obtained will have to be supported by a more extensive campaign of experiments, both real and numerical.

The performed preliminary numerical simulations are based on a simple but effective model that incorporates structural, non-structural and new components and, in addition, some further boundary hypotheses have been assumed about the features of the retrofit system. In particular, the three main assumptions considered in the structural FE model are: (i) the connections that bind the existing structural elements to the PC panels are infinitely rigid; (ii) the corresponding nodal degrees of freedom (DOFs) of infill RC frame, PC panel and filling RC concrete (in the plane, the two translations and one rotation) are constrained; (iii) IP behaviour is simulated, whereas OOP behaviour is neglected. While the condition (ii) retains a physical sense, due to the technology of the retrofit system, condition (i) is a strong assumption and it should be carefully assessed, because the failure of steel connectors affects the final performance (they must be specifically designed and verified). Nevertheless, some aspects can justify this assumption. In particular, the application of steel connectors exploits the technique of chemical anchoring, where before to insert the connector, a resin is injected into the hole. According to this technique, the chemical naturally fills in all irregularities and therefore makes the hole airtight and water proof, with high degree of adhesion (close to 100%). Still, the additional cast in-site lightweight structural RC layer inserted in the system allows to provide solidity to the whole package, by contributing with additional passive forces (e.g., friction) to the system's functioning. In the end, considering that the aim of the authors is to explore the overall global behaviour of the existing structures and the new precast panel system against horizontal actions, under an ideal situation of perfect system functioning, the assumption of infinitely rigid connection is given by a numerical necessity. Assessing local behaviour of the steel connections requires different investigation strategies, to observe the stresses and strains in each connection under extreme events. In this view, the simplified approach allows to explore what can be the contribute of the new system to the overall behaviour of the existing building. Also the condition (iii) needs some additional remarks. As a matter of fact, the retrofit system as conceived, interacts with the masonry infill panels as an additional structural system, creating a single vertical ribbed plate, connected to a RC frame structure. Assuming that the condition (i) is satisfied, the overturning of masonry panel under seismic action is prevented and then, condition (iii) can be considered valid.

Regarding to the numerical simulation, the FE model is conceived by referring to the proposal in Mondal and Jain (2008) and after revisited in Ozturkoglu, Ucar and Yesilce (2017), which studied the effects of the openings in the infill RC frames under seismic actions with a meso-scale approach. Using SAP2000 software (CSI, 2021), beams and columns are simulated as frame elements having in-plan three DOFs (two translational and one rotational), while infill panels are modelled as shell elements having in-plan two DOFs (two translational). The interface between frame and shell are simulated through rigid springs. Similarly, to the FE approach used for modelling masonry infill panels in RC frames, filling cast-in-place reinforced concrete (LWSC) and PC panel are simulated through shell elements having, the two nodal DOFs indicated in Figure 15. The three layers are linked among them through rigid springs to constrain the DOFs of all internal and external shell nodes. Still, Figure 15 shows a schematic representation of the numerical model.

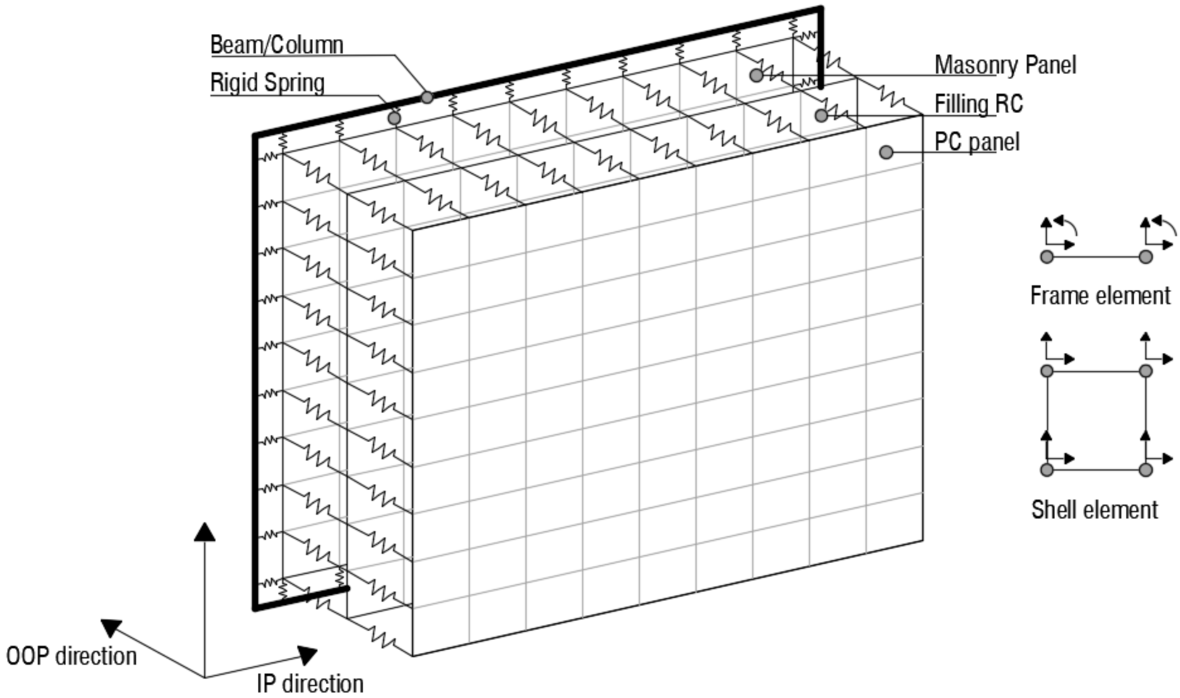

Figure 15 – Schematization of the proposed FE structural model and available DOFs for frame and shell elements.

The external restraints are simulated through fixed supports applied at the base of columns and simple supports at the base of meshed shell nodes, assuming the foundation (including the existing and the new one added for the retrofit technique) as rigid. Concerning to the nonlinear behaviour, a fiber approach has been implemented. Frame elements are modelled through the “section design” tool, by assigning the constitutive laws of concrete (confined and unconfined assumptions, as in Mander, Priestley and Park, 1998, Figure 16-a)) and steel rebar to each fiber of beams and columns and the resultant fiber hinges are located at the end sections of frames. Shell elements are characterized through “layered nonlinear shell” tool, by defining the geometry of the three package components and by assigning to each fiber the related constitutive law. Regarding to masonry infill panel, each fiber is modelled according to the constitutive law proposed by Kaushik, Rai and Jain (2007), Figure 16-b), while, for PC panels and filling cast-in-place RC the unconfined Mander constitutive law is implemented. Since no experimental data are available for a validation of the effectiveness of this proposal under seismic actions, especially for the masonry infill frame configuration, the results obtained by the numerical model are initially compared with the ones obtained by adopting the consolidated macroscale approach (Uva et al., 2012), which consists in the simulation of the masonry panel behaviour with a single strut that links opposite joints. The nonlinear behaviour of the strut for employing the macroscale approach has been simulated by using an axial plastic hinge, accounting for the Panagiotakos and Fardis constitutive law (Panagiotakos and Fardis, 1996), Figure 16-c) and by considering the elastic properties through a strut section defined according to Shing and Mehrabi (2002). Then, to investigate the seismic behaviour of the developed prototype, four numerical models have been developed, subjected to a nonlinear static analysis approach: (1) Bare frame model; (2) Infill frame model, by using a macro-scale approach; (3) Infill frame model, by using a meso-scale approach; (4) Retrofitted model, with multi-layer shells.

The results of the numerical analyses are shown in Figure 17, where two graphs are reported. The first one shows the comparison between bare and infilled frame models in terms of base shear (V_b) vs. roof displacement (δ_R). In the second graph, the comparison is made for the bare, infill with mesoscale and retrofit models.

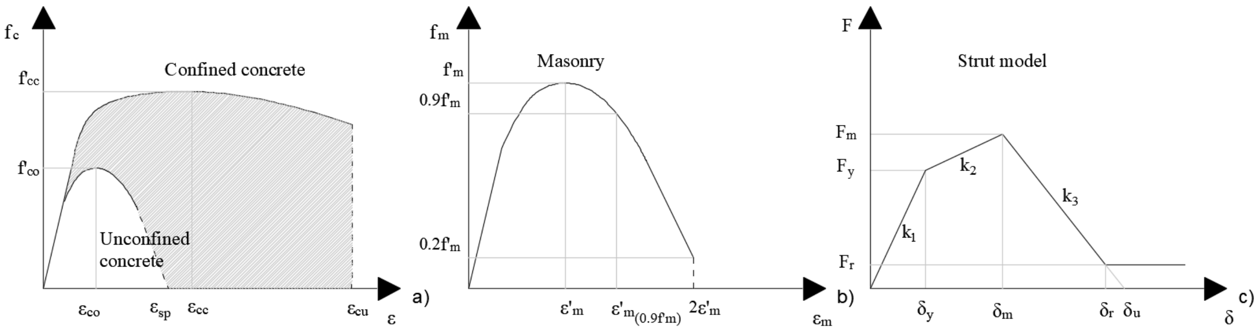

Figure 16 - (a) Constitutive laws of confined and unconfined concrete (Mander, Priestley and Park, 1998); (b) constitutive law of meso-scale (Kaushik, Rai and Jain, 2007) and (c) macro-scale (Panagiotakos and Fardis, 1996) models for masonry infill. All symbols are reported in the abovementioned references.

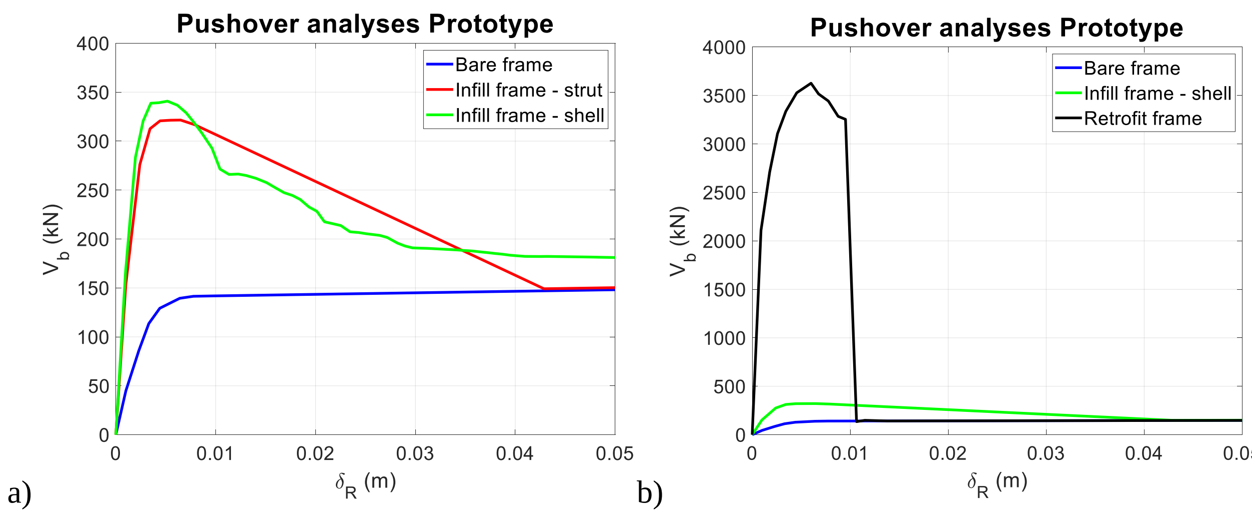

Figure 17 – Pushover analyses on prototype FE model: a) comparison among bare and infill frames with strut and shell models; b) comparison among bare, infill and retrofit frames elements.

Pushover results show that the assumption made for infill frames are in accordance (Figure 17a), with comparable values in terms of initial stiffness, peak V_b and δ_R and softening branch. Regarding to the retrofit method (Figure 17b), as expected, the results show the proposed methodology provides a high increment of initial stiffness and peak strength (about 10 times of the infill frame one) and a strongly reduced displacement capacity. As a matter of fact, in terms of seismic behaviour, this system shows a low ductility capacity (also negligible), especially in the post-yield branches. On the other hand, the high stiffness and strength contribution allows to assimilate the entire system to an elastic RC wall, with the related benefit in energetic retrofit terms. From the numerical point of view, when the failure of the masonry and retrofit layers is attained, the pushover curve re-joins to the one of the bare frame model, even if at this point the entire system could be considered as collapsed. Of interest is the behaviour of the system after reaching the peak capacity, where a short branch showing softening occurs before a definitive collapse of the curve. This implies that under horizontal loading, the stiffer layers take a higher contribute of the force than the bare frame model and then, they achieve almost simultaneously the collapse before than the frame.

5. Application of the proposed retrofit to a real case study building: numerical simulation

The methodology employed to design the IPCS, as the technological proposal for the energy and structural retrofit of the existing RC buildings in the South of Italy, has been applied to a case study to preliminarily assess the global structural response of the system on the specific type of building considered. In this section, both thermal and seismic behaviour of the building have been studied, with further investigations on specific portions. As abovementioned, all the analyses have been carried out basing on the approach defined by FE modelling, since no experimental tests have been performed. At this point, it is worth mentioning that on the selected case study, all the analyses and the numerical elaborations are aimed to assess the efficiency of the proposed approach, by completely neglecting the necessary phases for a reliable seismic assessment of an existing building (e.g., complete knowledge of the building through in-situ characterization of structural materials and structural elements, assessment of the constructive details).

With regard to the case study, the building analysed is part of the residential housing complex in the west-side of Trani, a city few km far from Bari. It is located in a peripheral zone along a wide street. It was constructed between 1958 and 1963 and contains most of the peculiar traits of the post-WW2 buildings in the South of Italy, remained almost unaltered over the years. It has been designed according to the older Italian code, only accounting for gravity loads and not considering any anti-seismic rules. Figure 18 shows a photo of the case study building.

Figure 18 – Case study building.

In detail, it is an MFH, regular in-plan and in-height, presenting a rectangular shape of 21.8 m x 10.9 m, two storeys of 3 m height (H), and moment-resisting frames in one direction, with a central staircase. Beam and column sections do not present variations between first and second floors and footings connected by beams constitute the foundations. Both storeys present RC ribbed slab, as in the greater part of the Mediterranean buildings, having constant joists of fixed dimensions (height 20 cm, width 10 cm, and spaced 50 cm) interspersed with hollow clay masonry blocks, all covered by a RC concrete layer of 4 cm thick. The infill walls are in hollow brick of 25 cm x 25 cm x 12 cm, casted in place with Portland cement 325 and quarry sand mortar. No insulating layers are included; thus, the U-value of the wall is 1.25 W/m^2K. From a visual inspection of the building, the windows have open-joint aluminium frames, with single glass and no insulating chamber. Figure 19 illustrates some examples of window surveyed.

With regard to the structural frame, Table 8 provides information about gravity loads (dead and live ones, respectively indicated with G and Q), information for the estimation of the seismic loads (coordinates (Lat, Lon), nominal life (N_L), usage class (U_C) and indexes of soil category and topography (Cat and Top)). Table 9 shows the hypothesized mechanical parameters of the elements (typical for the existing buildings of the focused geographic zone), i.e., mean compressive strength of in situ concrete (f'_{cm}), mean tensile strength of steel rebars (f'_{ym}), elastic modulus of concrete (E_c) and elastic modulus of reinforcement steel (E_s). The values of typical mechanical parameters of masonry are provided (e.g., Uva et al., 2012), such as the elastic moduli E_w, $E_{w\theta}$ and G_w, respectively, vertical, diagonal and shear ones, the compression strength σ_m and the tensile strength f_{tp}. The characteristics of the elements are summarized in Figure 20, wherein there are beams and column sections and the related steel reinforcement.

Table 8 – Report about case study building: loads and geometrical information

Gravity Loads			Height	Seismic loads					
G_1 (kN/m^2)	G_2 (kN/m^2)	Q (kN/m^2)	H_1=H_2 (m)	Lat (°)	Lon (°)	N_L	U_c	Cat	Top
3.50	2.50	2.00	3.00	16.416	41.274	50	1	C	T_2

Table 9 – Report about case study building: mechanical parameters

In situ Concrete		Steel Rebar		Masonry Elements				
f'_{cm} (MPa)	E_c (MPa)	f'_{ym} (MPa)	E_s (MPa)	E_w (MPa)	$E_{w\theta}$ (MPa)	G_w (MPa)	σ_m (MPa)	f_{tp} (MPa)
20.00	29962	440.00	205000	3080	1495	1233	2.5	0.36

Figure 19 – Case study building: survey of the windows.

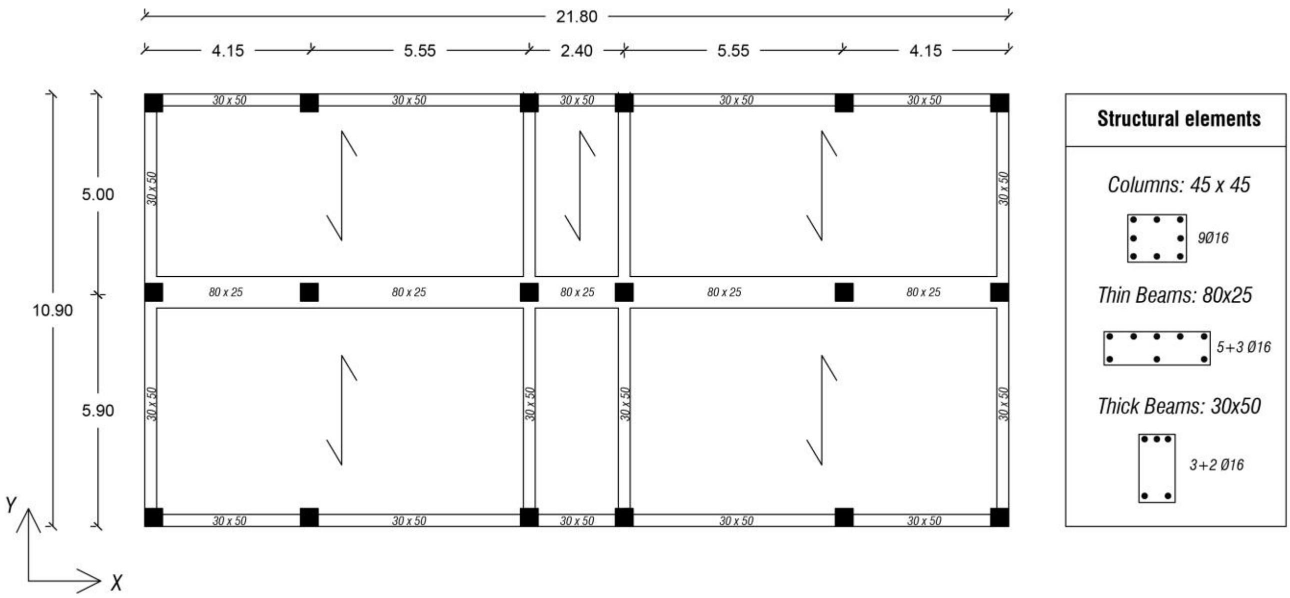

Figure 20 - Structural scheme of the case study and detail of end sections of structural elements.

5.1. Assessment of the thermal behaviour improvement: analyses and results

The considered case study presented the wall typology of the most common RC building constructed in the post-WW2 in the South of Italy. It corresponds to the building façade chosen for the development of the IPCS design methodology. Therefore, the U-value of the wall has been considered equal to 1.25 W/m^{2}K since no insulation layer was included into the section. The analysis of the current state of the building was performed according to the methodology in the Section 4.3 with the mean Trani's climate conditions below, selected from Bari Karol Wojtyla weather station, Italy (WMO: 162700) by ASHRAE Climatic Design Conditions 2003/2013/2017 (subscripts *i* and *e* indicate internal and external, respectively):

- $T_i°$= 293.15 K; RH_i = 52%.
- $T_e°$ = 281.55 K; RH_e = 68%.

The thermal behaviour was observed through a qualitative approach using the software COMSOL Multiphysics in steady-state conditions. The details of the FE model are summarized as follows: calibration for general physics; maximum element size: 3.86E-4 m; minimum element size: 6.95E-5 m; maximum element growth rate: 1.5; curvature factor: 0.6; resolution of narrow regions: 0.5. The heat flux in a specific building portion was deepened. Hence, a reduced model of the building which contained a half part of the balcony/loggia between two apartments was imported in the software and Figure 21 shows the considered building portion from the outside (a) and inside (b) in the FE environment. The two views were called OUT and IN, respectively. Figure 22 illustrates the results of the analysis of the building actual state, in the plan view, while Figure 23 in OUT view (a) and IN view (b).

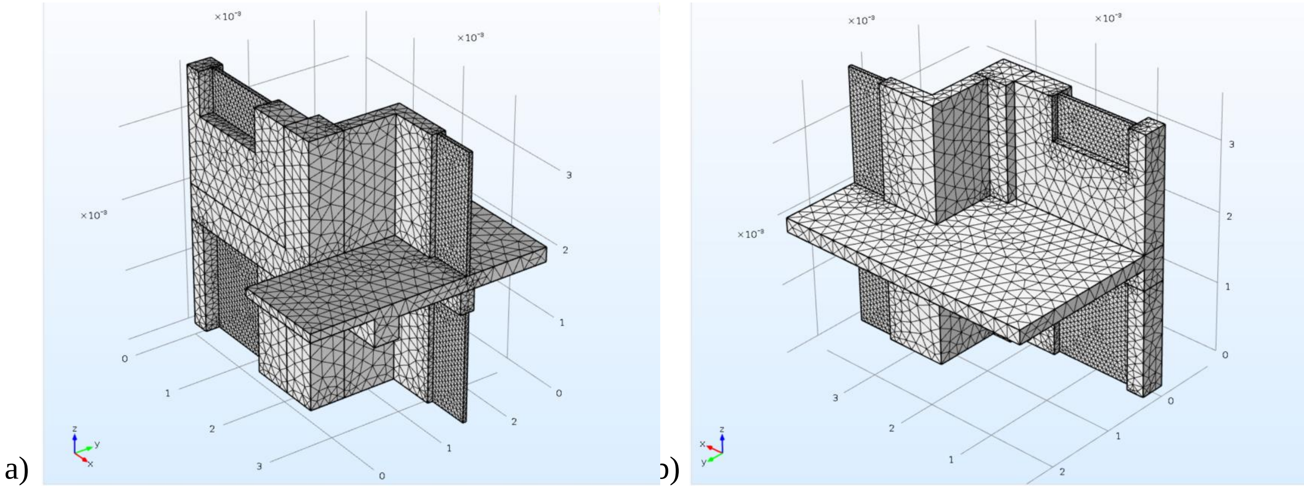

Figure 21 - Thermal behaviour assessment: building portion in FE environment a) from outside; b) from inside.

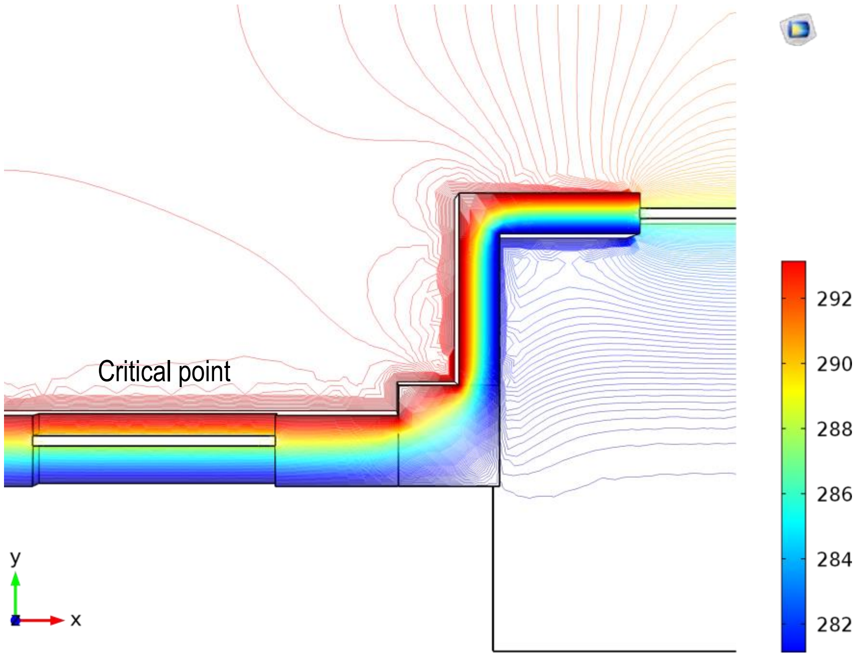

Figure 22 – Thermal behaviour assessment - actual state: plan view.

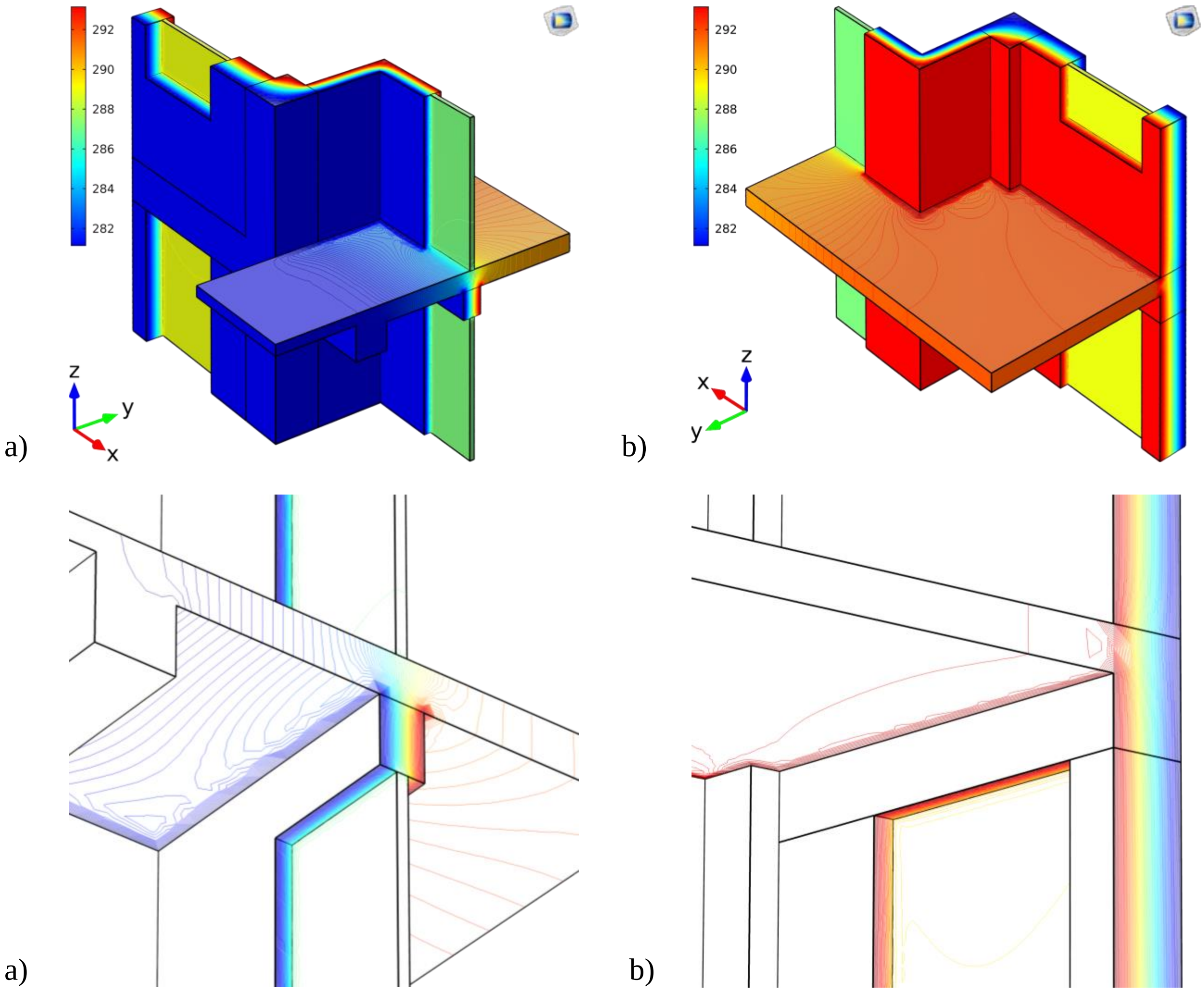

Figure 23 – Thermal behaviour assessment - current state a) OUT view; b) IN view.

At the current state, the temperature difference between the inner and outer faces of the building was about 11.4 K. It generated a great outgoing thermal flux with heat losses of about 70% in the section. It was accentuated at the intersections between the wall and the balconies, especially in correspondence of the windows. Thermal bridges were not surveyed due to the thickness of the external walls. Although, a critical point was identified at the junction between the column and the thinner wall of the lodge in the indoor corners. Therefore, the simulation of the refurbishment through the novel system was performed. Since the pilot building had the same characteristics of the model employed to explain the methodology and the climate conditions were similar to those for the characterization of the IPCS, the preliminary analysis about thermo-hygrometric behaviour is similar to the one above explained. Instead, the heat flux and the thermal bridges assessment was conducted in order to understand the effectiveness of the system in preventing thermal dispersions. Since the simulations have regarded only the retrofit of the external walls, the windows and the other aspects have been leaved unaltered. Therefore, among the results, an excellent thermal insulation capacity is expected from the new system but a strong thermal dispersion on the surfaces of the windows that are not equipped with any protection. Figures 24 illustrates the results a) global behaviour; b) global section X-Y view; c) section X-Y (window); while Figure 25 illustrates the results d) section Y-Z (wall-windows); e) section Y-Z (wall).

The overall behaviour of the building portion with the application of the IPCS system is extremely satisfying. The walls stay warm almost along the whole section with temperature difference between the inner and outer side of about 3 K and a reduction of the heat losses of about 74%. However, as expected, in correspondence of the windows, the heat flux became irregular with a huge temperature variation at the intersection with the system, between the insulating wall and the external coating.

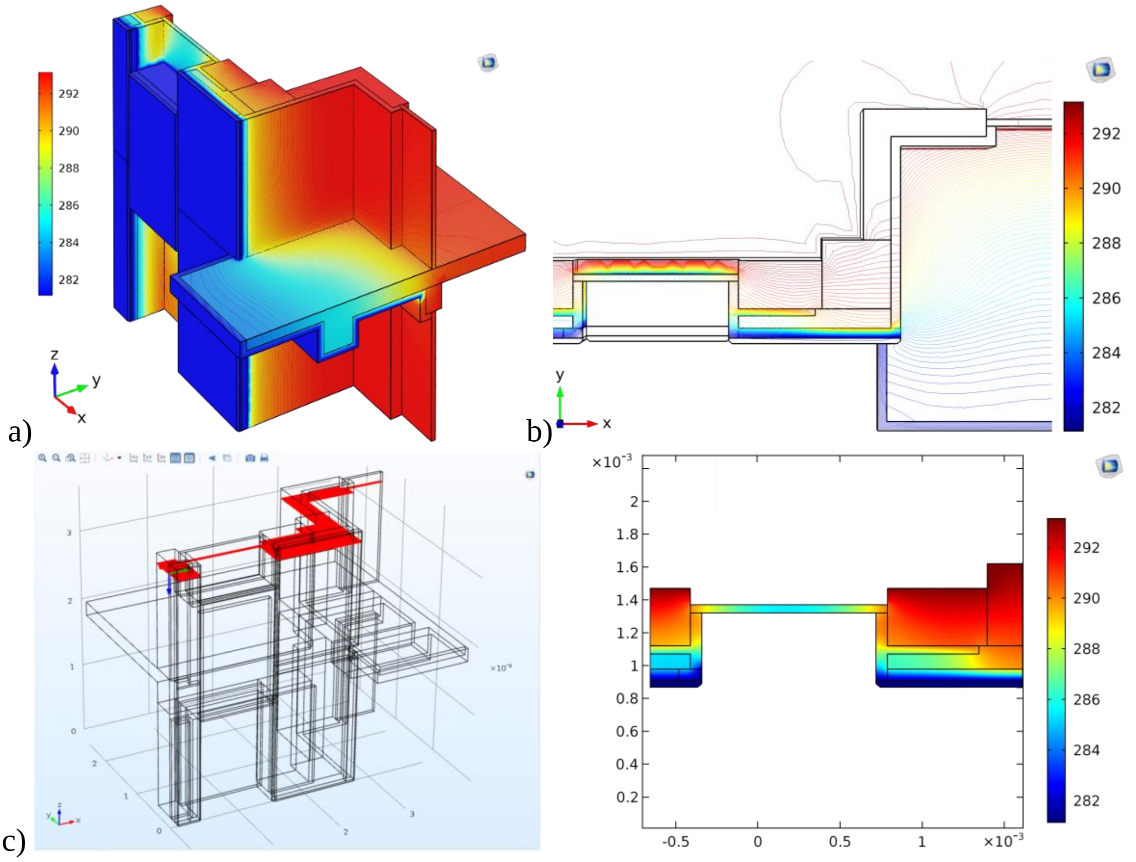

Figure 24 – Results of the visual analyses of the system thermal advances: a) global behaviour; b) global section X-Y view; c) section X-Y (window).

The windows caused a high dispersion of heat, also affecting the performance of the system and the outer coat. In addition, the presence of different materials in the section of the building, e. g., the concrete of the beams and the ceramic of the brick wall, generated an uneven distribution of temperature in the upper and lower part of the wall. It was due to the presence of a thinner outer lining insulation layer. A thicker insulation panel would solve this problem.

d)

e)

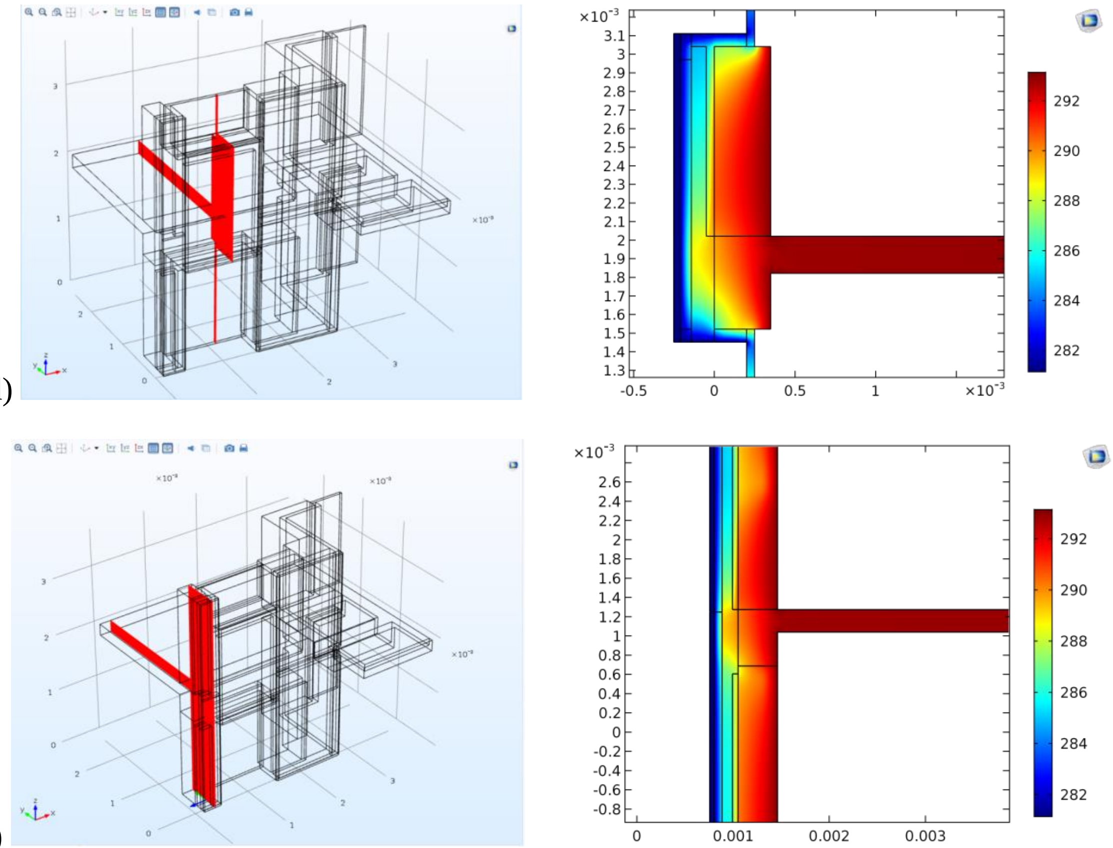

Figure 25 – Results of the visual analyses of the system thermal advances: d) section Y-Z (wall-windows); e) section Y-Z (wall).

5.2. Seismic behaviour assessment: analyses and results

The case study building has been modelled by using SAP2000 software (CSI, 2021). According to the methodology employed for the prototype FE model in the Section 4.4, a fiber approach has been implemented. In particular, nonlinear behaviour of frame elements has been defined by assigning fiber hinges at the beams and columns end sections through “Fiber P-M2-M3” library, while shell and link elements are defined as for the prototype model. For the structural performance estimates, eight FE models have been developed (four configurations in the 2 main directions, X and Y, as defined in Figure 20), by considering bare frame (BF), infill with masonry panel simulated with shell elements (IF) and two retrofit configurations (RF1; RF2). The differences between RF1 and RF2 are related to technological aspects in the application of PC panels on an existing RC building. In particular, RF1 consists in the application of the proposed retrofit technique only on the filled parts of the building envelope and by neglecting the parts in correspondence of the openings; RF2 consists in the application of the retrofit on the entire building envelope, in the hypothesis that PC panels can be resized in order to accommodate all openings (both windows and doors). In the practice, both solutions included in RF1 and RF2 could be employed. For sure, RF1 results to be the easier way to apply the PC panel, considering the vertical connections and the possible presence of balcony, which can interrupt the desired interaction. On the other hand, for achieving a full energetic retrofit, it is necessary to forecast a thermal coat on the uncovered parts of the building envelope. RF2 represents the best way to obtain an elevate performance from the energetic and seismic point of view, but it could hold some difficulties in the PC panel application, due the assignment of an irregular shape to PC panel and the related connections with the structural elements. Assuming a prefect feasibility of the retrofit about technologic and structural local aspects, all numerical models present columns fixed at the base, while shells simulating masonry panels are restrained at the base with simple supports. An internal constraint has been predisposed for simulating a rigid diaphragm, which can represent a correct assumption in the case of perfect box behaviour. Loads G and Q are applied as distributed on the frame elements, according to the seismic combination provided by the Italian Building Code (2018). Regarding to shell elements, both in infill and retrofit configurations, the presence of openings for doors and windows have been accounted. Concerning to the ductile and shear capacities of elements, the automatic definition of the nonlinear properties of frames and shells allows to fix the trend of failure mechanisms on the stress-strain behaviour of the several materials employed. In particular, concrete fibres are characterized with an unconfined Mander constitutive law, while steel fibres are modelled with an elasto-plastic constitutive law with hardening behaviour. At the same time, the acceptance criteria for defining the achievement of the limit-states for frame elements have been automatically defined.

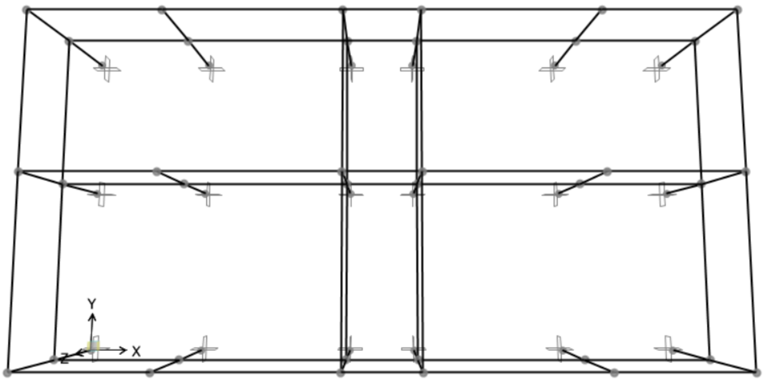

3D view - BF Model (Same for X and Y directions)

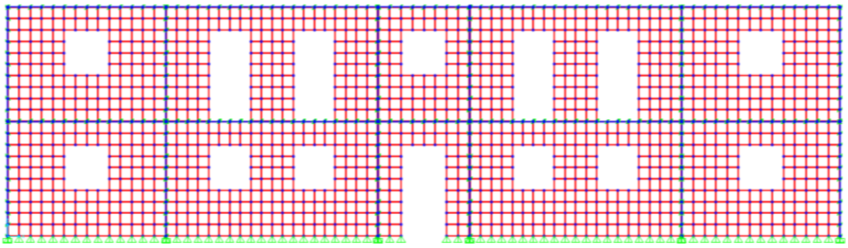

Plane X-Z - IF Model (X direction)

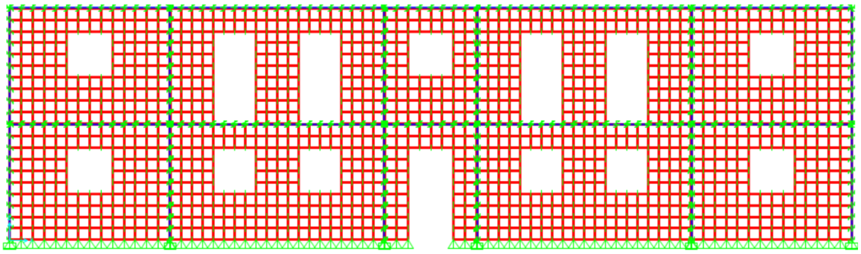

Plane X-Z – RF2 Model (X direction)

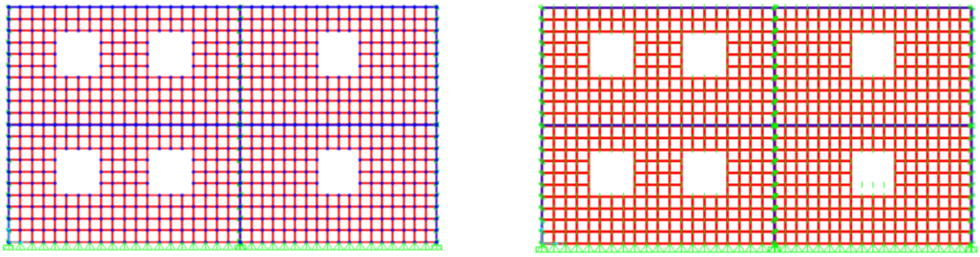

Plane Y-Z - IF Model (Y direction) Plane Y-Z – RF2 Model (Y direction)

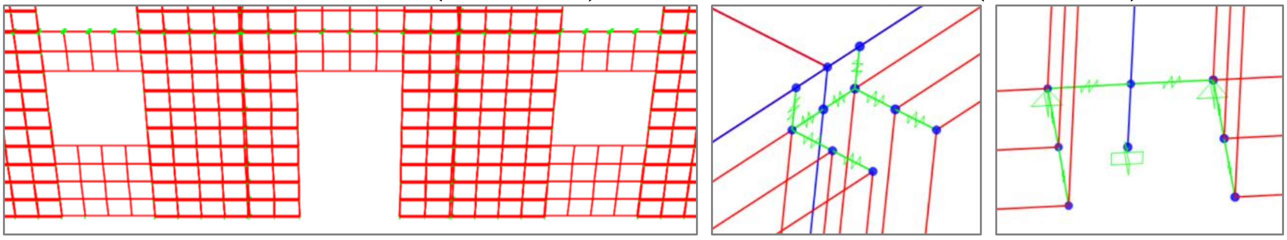

3D view - FE models details: particular of RF1 model and link among shell and frame elements

Figure 26 – Numerical models for seismic evaluations and FE model details.

Looking at the concrete stress-strain, the life-safety (LS) limit-state is defined for a strain value of fibres equal to 0.20%; the near collapse (NC) limit-state is defined for a strain value of fibres equal to 0.35% according to the limits provided by the Italian Building Code, 2018; the immediate occupancy (IO) limit-state is defined as a percentage of the above strain value. Figure 26 shows a summary of the eight numerical models, where images are subdivided for the two main directions, besides to report some modelling details regarding to the link among frame and shell elements. It is worth noting that the shell elements have been meshed, according to the schematization proposed in Figure 26, by assuring that the results obtained with a fitter mesh presents a maximum scatter of 3% and by linking each joint with perpendicular rigid link.

After, eigenvalue analyses have been carried out on the eight numerical models. Table 10 reports main periods (T) and the related participation mass (M[%]) per direction. As expected, going from the BF model to IF, RF1 and RF2 configurations, the *T* values reduce and the same evidence can be noted for M[%]. The complexity of retrofit numerical models leads to shift the main mode per direction to the higher ones. Nevertheless, these expected effects do not push the M[%] values under the thresholds of 75%, which means that according to the provisions by the Italian Building Code (2018), the nonlinear behaviour of all models can be investigated with unimodal pushover analysis.

Table 10 - Main periods and participating masses for the numerical models of the case study building

Numerical Model	T (s)	M[%]
BF – X	0.242	85.92
BF – Y	0.307	88.28
IF – X	0.115	84.45
IF – Y	0.15	85.18
RF1 – X	0.030	77.53
RF1 – Y	0.037	81.65
RF2 – X	0.027	76.54
RF2 – Y	0.035	80.95

Accordingly, unimodal pushover analyses were performed on the eight numerical models and the results can be displayed in Figures 27 and 28, by assuming as control node the centre of the mass of the last storey, by neglecting any sources of eccentricity and by representing the resultant curves in terms of V_b-δ_R.

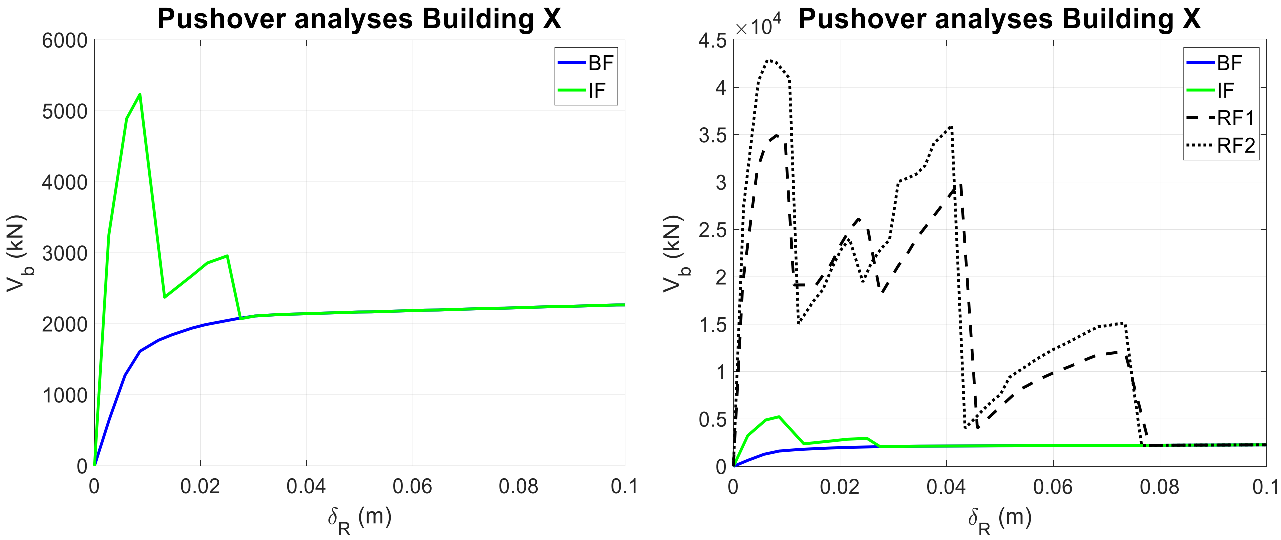

Figure 27 – Pushover analyses in X direction for bare (BF), infill (IF) and retrofit configurations (RF1 and RF2).

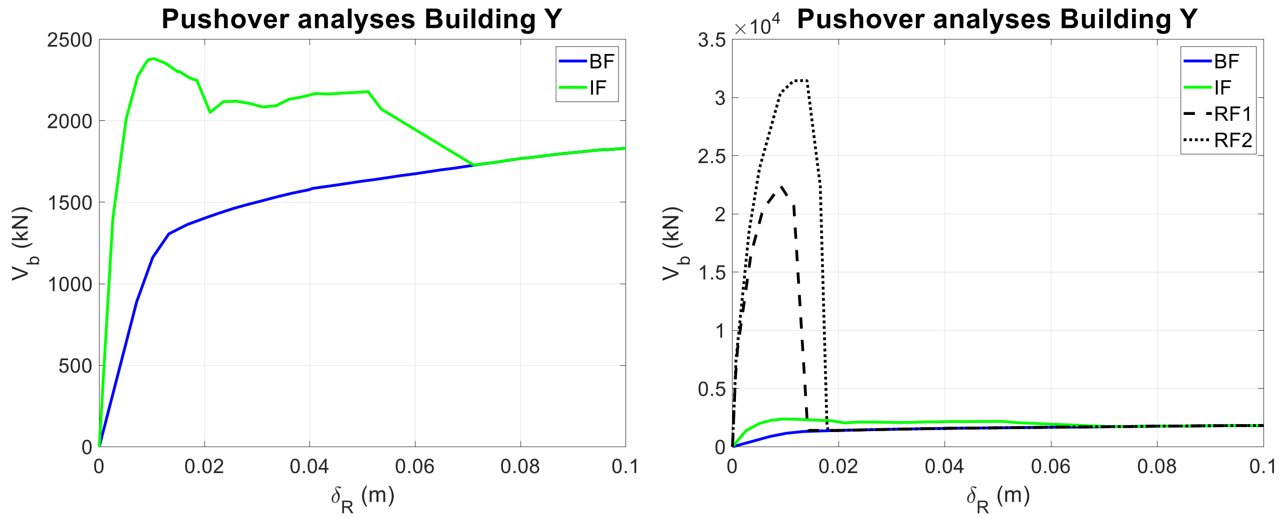

Figure 28 – Pushover analyses in Y direction for bare (BF), infill (IF) and retrofit configurations (RF1 and RF2).

As expected, the pushover curves show that IF models in both main directions (left graphs in Figures 27 and 28) present an initial peak which after returns on the BF model trend. For infill models, the numerical complexity given by the shell elements employment provokes a “Saw-Tooth” trend, due to numerical convergence problems. Similar effects can be shown by the comparison among the previous curves and RF1 and RF2 (right graphs in Figures 27 and 28). Especially in X direction, pushover curve shows some resurrections, also due to the presence of a large set of openings. In the Y direction this effect did not occur, probably because the openings surface is reduced. The total collapse of shell elements (more rigid than the frame) occurs before than moment-resisting frame and bring back the curve on the BF trend, as well as displayed for IF model. Comparing the results obtained for RF1 and RF2, it is evident the slight difference in term of strength, especially around the peak values in both directions. In terms of δ_R, RF1 shows a similar capacity in X and a lower one in Y. These results suggest that, from the global structural performance point of view, both RF1 and RF2 provide similar behaviour in terms of strength, stiffness and ductility and the possible advantages for both methods are mainly related to technological aspects. Also in this application, as highlighted for the prototype model, this retrofit technique increases the stiffness and the strength of the structural system, with a peak V_b of about 10 times (in the case of RF2) the IF value. On the other hand, the deformation capacity and the related ductility is strongly reduced, which means that the building behaves like an elastic (or low-ductile) structural system.

From the physical point of view, the obtained results need of some interpretations. As a matter of fact, the resurrections occurred in X direction are the result of a numerical elaboration, but at the first significant strength loss, the retrofit system could be declared as collapsed. At the same time, considering that the real interaction between the frame and the added PC panels is rigid, a strength decay effect could lead some structural elements to achieve their strength capacity limits. Then, in a conservative view, the achievement of the LS limit-state (NC also, the two limit-states can be confused in this case) for RF1 and RF2 is signalled at the first significant strength decay shown by pushover curves. For the same reasons, in this case it does not physical sense to establish a criterion for defining the violation of the IO limit-state. For the other structural configurations (BF and IF), the limit-states definition can be assumed in a practice-oriented view, such as summarized in Ruggieri et al. (2021). More in detail, LS limit-state is achieved when shear failure appears in any element or when certain percentage of elements achieve the 75% percent of the ultimate rotation (in this case, the ultimate rotation is automatically defined from the moment-rotation law of each section); IO limit-state is achieved at the 0.5% of the inter-storey drift ratio for the bare frame configuration and at the displacement on pushover curve correspondent to the first significant strength loss for the IF configuration. The limit-states thresholds, as above defined and as reported in Table 11, show that going from BF to IF and after to RF1 and RF2, the IO and LS values of δ_R decrease, caused by the stiffness and strength variations among the models. The definition of these limit-states thresholds is necessary for the comparison of the building capacity (in all simulated configurations) and the seismic demand, which represents the standard procedure of global seismic assessment, according to Eurocode 8 (for more details, see Ruggieri and Uva, 2020). For the case at hand, the assumption of δ_R like engineering demand parameter to determine the transition to a higher damage state is due to the nature of our evaluations, which is aimed to identify a global performance and, to the nature of the analysis method performed. Assuming as seismic demand the code spectra for the IO and LS limit-states and comparing them with the capacity curves, opportunely scaled to the single DOF system, it is possible to compute the capacity/demand (C/D) ratios.

Table 11 - Values of IO and LS limit-state thresholds, for all FE models, in terms of δ_R

Numerical Model	IO - δ_R (m)	LS - δ_R (m)
BF – X	0.0183	0.0373
BF – Y	0.0205	0.0389
IF – X	0.0089	0.0171
IF – Y	0.0133	0.0210
RF1 – X	/	0.0131
RF1 – Y	/	0.0152
RF2 – X	/	0.0112
RF2 – Y	/	0.0149

The results are plotted in Figure 29, where the C/D ratios are always greater than 1, which means that for the seismic demand considered the building is always verified. Still, from the C/D ratios evaluation, it is worth noting that the obtained values for RF1 and RF2 are strongly greater than the related values obtained from the BF and IF models, for both main directions. For example, in X direction RF2 presents a C/D ratio value about 15 times greater than of the IF value. Despite this benefit is not obtained in terms of displacement capacity (or in terms of ductility), it is clear that the stiffness of RF1 and RF2 causes low values of periods, which somehow reduce the seismic demand (the mass increases, but in a lower measure than stiffness). This means that the proposed retrofit method allows to obtain strongly higher safety levels for the entire structural system than the IF configuration.

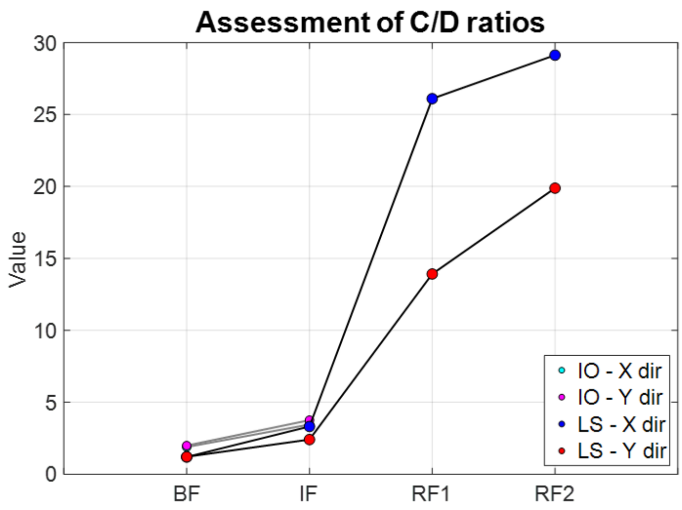

Figure 29 – C/D ratios for all models, for IO and LS limit-states and for both main directions (X and Y directions).

In the end, to validate the results of pushover analyses, nonlinear response history analyses (NRHAs) were performed on the models simulating the building under all structural configurations. To this scope, a record selection was performed through the tool Rexel (Iervolino et al., 2010), employing the Eurocode 8 provisions. In particular, differences between mean and target spectra amounted to +30% and –10%, while the fitting was performed between 0 and 0.6 s (two times of the maximum period among the ones recorded for all models). Figure 30 shows graphs reporting the set of 14 elastic ground motions spectra (grey lines), the obtained mean spectrum (black line) and the considered target spectrum (red line), all for 5% damping (Sa_e indicates the elastic acceleration).

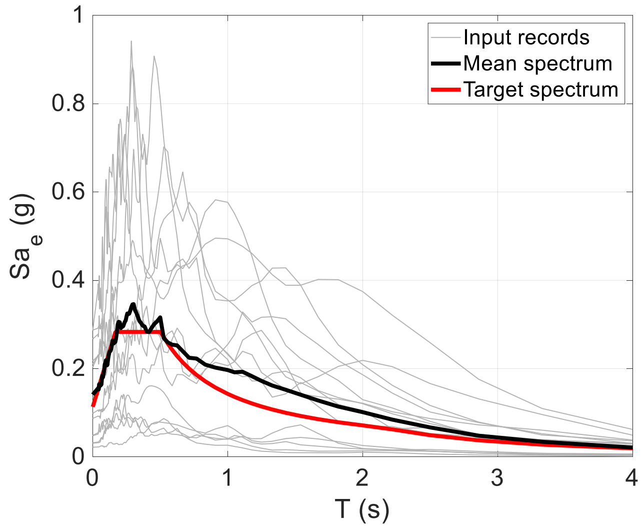

Figure 30 - Elastic acceleration spectra of the set of ground motion records, mean and target spectra (5% damping).

Using the selected records, NRHAs were performed on all models and results in terms of δ_R vs. V_b were compared with pushover analyses, as shown in Figure 31. Looking at X direction (the more vulnerable direction from pushover analysis and C/D ratios), for BF and IF models, 5 ground motion records provide responses in the elastic/yielding part of the curves (black points), while 2 ground motion records provide collapse of the building (red points placed at the right hand of the graphs and with the last recorded V_b before the collapse). Instead, on RF1 and RF2, the results of NRHAs show how all points are located on the elastic branch of pushover curve, without exceeding the elastic limit. Comparing the overall behaviour of the retrofitted building with IF and BF models, the value of V_b increases, evidence mainly due to a substantial increment of mass. On the other hand, as expected, the increment of stiffness provides two main benefits: (a) the decrease of the fundamental vibration periods and then, the reduction of acceleration (spectral acceleration is coming close to PGA values); (b) the displacement demand is strongly reduced.

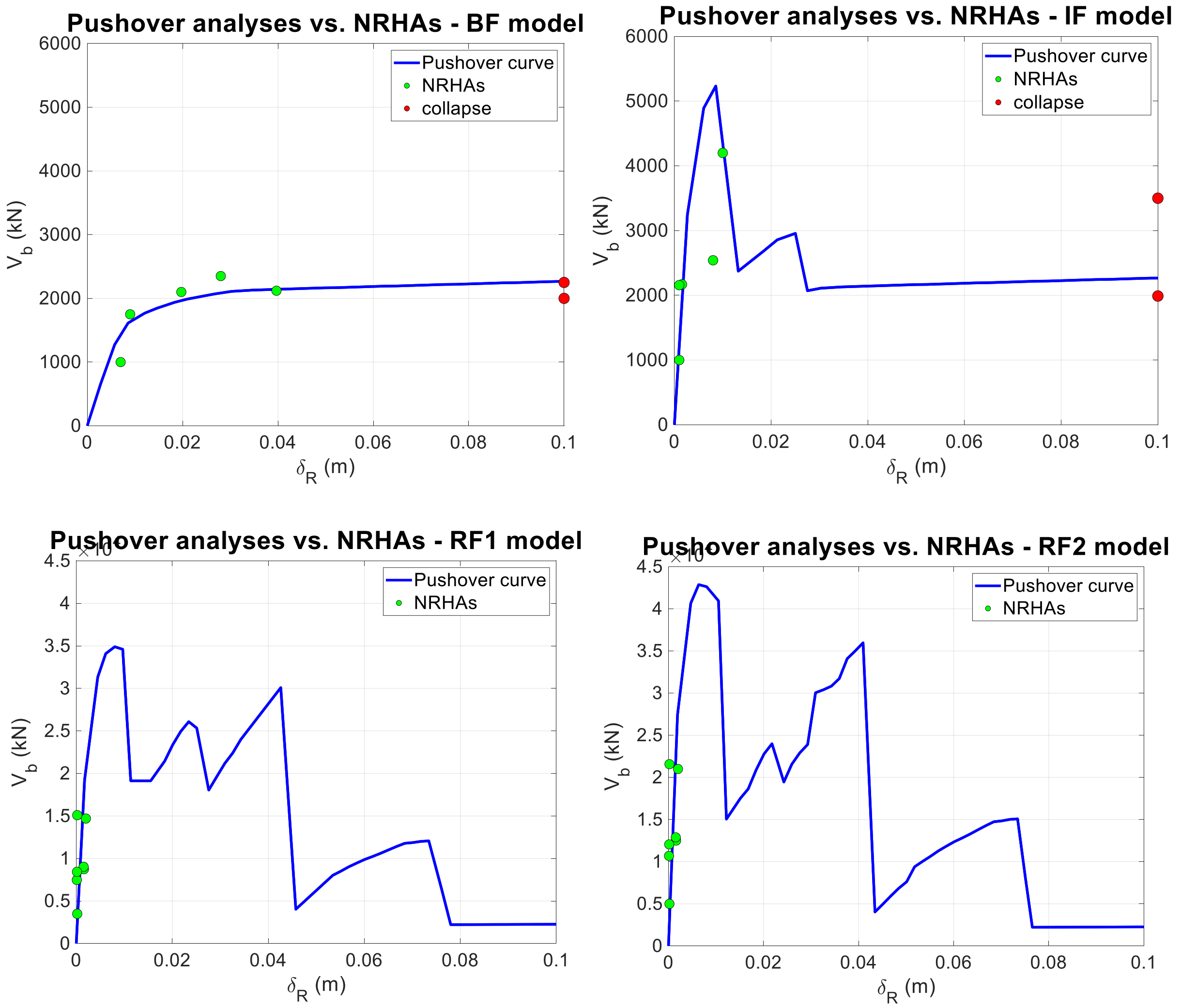

Figure 31 - Comparison of pushover curves with results by NRHAs for BF, IF, RF1 and RF2 models. Red points indicate collapse and are placed at the right hand of the graph.

Finally, as mentioned in the first part of this Section, the global seismic assessment presented does not take into account of some key aspects that should be always considered in this kind of analysis. In particular, in the case study, even if existing structural elements have been considered to obtain the global response, the specific capacity assessment (in terms of resistance, ductility and stiffness) of structural and non-structural elements is not performed, as well as the design and verification of the connections that ensure the working of the entire system and the necessary adjustment to make on the existing foundation. Overall, the retrofitted building will work as a dual frame-wall system, in which seismic actions are mainly entrusted to by the new wall system. Anyway, it is not possible to state that the building is completely safe toward seismic actions only basing on the presented analyses. Albeit several assumptions have been made in the definition of the system and in its numerical model, the general approach shows a good potentiality of the proposed technique as an efficient retrofit system.

6. Conclusions and further developments

The paper presents an explorative study on a retrofit system consisting in a precast concrete panel integrating recycled materials, designed for the twofold scope of improving energetic and structural performance of existing buildings that date back to the post-World War. In particular, the new system is designed to improve the thermal insulation of the buildings by means the external application of the new system on the building façade and to strongly increase strength and stiffness of the focused building, varying the structural behaviour against horizontal actions and avoiding potential failures of structural and non-structural elements. About the proposed retrofit system, a detailed description of the technological procedures for its real application is provided, assessing the real feasibility of the method by means of a real-scale prototype. Still, in order to assess both energetic and seismic performance improvements, separate analyses have been conducted, taking as reference the prototype, which anyway has been not experimentally tested. Despite several initial assumptions have been fixed, from the energetic point of view several scenarios of wall stratigraphy have been tested through finite element analyses, in order to achieve best solutions to improve aspects as hygrometric behaviour and thermal bridges formation. From the structural point of view, a finite element model has been predisposed, as based of a meso-scale approach able to simulate the interaction among the existing infilled frame, the new panel and the interposed filling lightening reinforced concrete. Later, both numerical techniques have been applied on a real case study, for which both energetic and structural analyses provided results showing good performances of the approach.

Obviously, this explorative study and the obtained results shall be assessed with proper experimental campaigns, able to provide real responses of the energetic and structural performances of the IPCS, as the base for future numerical simulations and marketing. Especially from the structural and seismic point view, several limitations of the proposed system must be highlighted. As a matter of fact, the application of the new panels strongly increases the mass of the existing building (besides to the stiffness) and, under seismic actions, this mass is transferred to the existing frame through the steel connectors and the frictional forces provided by the filling RC layer. Hence, a detailed designed of the steel connector must be carried out (e.g., size of connectors, spacing, type of chemical anchorage). Even with regard to numerical simulations, all the simplified assumptions must be accurately assessed, considering that steel connectors are not infinitely rigid and then, the local behaviour must be accounted for. Despite the above limitations, Nevertheless, the methodologies here presented have shown comforting potentialities and interesting insights of the methodology, which open new perspectives in the use of these types of systems on existing buildings.

Data Availability Statement

Some or all data, models, or code that support the findings of this study are available from the corresponding author upon reasonable request.

References

2nd SKIN zero energy apartment renovation via an integrated façade approach, Final Public Report Project within the subsidy program Energy & Innovation, TKI/ENERGO Reference Number TEGB 113029 (2016). (accessed December 4, 2021)

Abruzzi Region price list of building works and interventions (2022), https://www.regione.abruzzo.it/content/nuovo-prezzario-regionale

Aguerre, J. A., Konstantinou, T., Klein, T., Steensma, S., Santin, O. G., Silvester, S. (2017). Investigating the business case for a zero-energy refurbishment of residential buildings by applying a pre-fabricated façade module. In ECEEE 2017 Summer Study on energy efficiency: Consumption, efficiency and limits (pp. 1113-1122). European Council for an Energy Efficient Economy (ECEEE).

Akin, A., Sezer, R. (2016). A study on strengthening of reinforced concrete frames using precast concrete panels. KSCE Journal of Civil Engineering, 20(6), 2439-2446.

Annex, I. E. (2011) Prefabricated Systems for Low Energy Renovation of Residential Buildings Retrofit Module Design Guide This report documents results of cooperative work performed under the IEA Programme for Energy Conservation in Buildings and Community. http://www.ecbcs.org.

Artino, A., Evola, G., Margani, G., Marino, E. M. (2019). Seismic and energy retrofit of apartment buildings through autoclaved aerated concrete (AAC) blocks infill walls. Sustainability, 11(14), 3939.

Asteris, P. G., Antoniou, S. T., Sophianopoulos, D. S., Chrysostomou, C. Z. (2011). Mathematical macromodeling of infilled frames: state of the art. Journal of Structural Engineering, 137(12), 1508-1517.

Baran, M., Okuyucu, D., Susoy, M., Tankut, T. (2011). Seismic strengthening of reinforced concrete frames by precast concrete panels. Magazine of concrete research, 63(5), 321-332.

Baran, M., Tankut, T. (2011). Retrofit of non-ductile RC frames with precast concrete (PC) wall panels. Advances in Structural Engineering, 14(6), 1149-1166.

Basha, S. H., Kaushik, H. B. (2019). Investigation on improving the shear behavior of columns in masonry infilled RC frames under lateral loads. Bulletin of Earthquake Engineering, 17(7), 3995-4026.

Belleri, A., Marini, A. (2016). Does seismic risk affect the environmental impact of existing buildings? Energy and Buildings, 110, 149-158.

Borodinecs, A., Zemitis, J., Dobelis, M., Kalinka, M. (2018). 3D scanning data use for modular building renovation based on BIM model. In MATEC Web of Conferences (Vol. 251, p. 03004). EDP Sciences.

Borodinecs, A., Zemitis, J., Dobelis, M., Kalinka, M., Geikins, A. (2017). Development of Prefabricated Modular Retrofitting Solution for Post-World War II Buildings.

In Environmental Engineering. Proceedings of the International Conference on Environmental Engineering. ICEE (Vol. 10, pp. 1-8). Vilnius Gediminas Technical University, Department of Construction Economics & Property.

Bournas, D. A. (2018). Concurrent seismic and energy retrofitting of RC and masonry building envelopes using inorganic textile-based composites combined with insulation materials: A new concept. Composites Part B: Engineering, 148, 166-179.

CEN (2004) Eurocode 3: Design of steel structures.

Choi, S. H., Hwang, J. H., Han, S. J., Joo, H. E., Yun, H. D., Kim, K. S. (2020). Seismic performance assessments of RC frame structures strengthened by external precast wall panel. Applied Sciences, 10(5), 1749.

Choi, S. H., Hwang, J. H., Lee, D. H., Kim, K. S., Zhang, D., Kim, J. R. (2018). Experimental study on RC frame structures strengthened by externally-anchored PC wall panels. Computers and Concrete, 22(4), 383-393.

COMSOL Multiphysics® v. 5.6. (2018) www.comsol.com. COMSOL AB, Stockholm, Sweden.

CSI SAP2000 (2021). Analysis Reference Manual', CSI: Berkeley (CA, USA): Computers and Structures INC.

D'Angola, A., Manfredi, V., Masi, A., & Mecca, M. (2019). Energy and seismic rehabilitation of rc buildings through an integrated approach: an application case study. In Green Energy Advances (p. 57). IntechOpen.

De Risi, M. T., Furtado, A., Rodrigues, H., Melo, J., Verderame, G. M., António, A., Varum H., Manfredi, G. (2020). Experimental analysis of strengthening solutions for the out-of-plane collapse of masonry infills in RC structures through textile reinforced mortars. Engineering Structures, 207, 110203.

Del Gaudio, C., Di Ludovico, M., Polese, M., Manfredi, G., Prota, A., Ricci, P., Verderame, G. M. (2020). Seismic fragility for Italian RC buildings based on damage data of the last 50 years. Bulletin of earthquake engineering, 18(5), 2023-2059.

Della Corte, G., Fiorino, L., Mazzolani, F. M. (2008). Lateral-loading tests on a real RC building including masonry infill panels with and without FRP strengthening. Journal of materials in civil engineering, 20(6), 419-431.

Di Domenico, M., Ricci, P., Verderame, G. M. (2019). Experimental assessment of the out-of-plane strength of URM infill walls with different slenderness and boundary conditions. Bulletin of Earthquake Engineering, 17(7), 3959-3993.

Di Perna, C., Stazi, F., Casalena, A. U., Stazi, A. (2008). Massa e comfort: necessità di una adeguata capacità termica areica interna periodica. Industria dei laterizi.

DM 17/01/2018 (2018) Aggiornamento delle Norme Tecniche per le Costruzioni. Gazzetta Ufficiale n. 42. February 20, Rome(In Italian).

DM 26/06/ 2015 (2015) Adeguamento linee guida nazionali per la certificazione energetica degli edifici. (In Italian)

Dobelis, M., Kalinka, M., Borodinecs, A. (2016, August). The Capture of BIM Compatible 3D Building Model from Laser Scanner Data. In The 17th International Conference on Geometry and Graphics (ICGG 2016): Abstracts, China, Beijing (pp. 4-8).

Dolce, M., Speranza, E., Giordano, F., Borzi, B., Bocchi, F., Conte, C., Di Meo A, Faravelli M., Pascale, V. (2019). Observed damage database of past Italian earthquakes: the Da. DO WebGIS. Bollettino di Geofisica Teorica ed Applicata, 60(2

Dolšek, M., Fajfar, P. (2001). Soft storey effects in uniformly infilled reinforced concrete frames. Journal of Earthquake Engineering, 5(01), 1-12.

El-Dakhakhni, W. W., Elgaaly, M., Hamid, A. A. (2003). Three-strut model for concrete masonry-infilled steel frames. Journal of Structural Engineering, 129(2), 177-185.

EN ISO 13786 (2018) Thermal performance of building components - Dynamic thermal characteristics - Calculation methods. http://store.uni.com/catalogo/uni-en-iso-13786-2018 (Accessed: 29 November 2020).

EN ISO 13788 (2013) Hygrothermal performance of building components and building elements - Internal surface temperature to avoid critical surface humidity and interstitial condensation - Calculation methods. http://store.uni.com/catalogo/index.php/uni-en-iso-13788-2013.html (Accessed: 12 April 2019).

EN ISO 6946 (2018) Building components and building elements - Thermal resistance and thermal transmittance - Calculation methods. http://store.uni.com/catalogo/index.php/uni-en-iso-6946-2018.html (Accessed: 12 April 2019).

European Commission, Energy efficiency first: accelerating towards a 2030 objective of 32.5%, Eu. Comm (2019). https://ec.europa.eu/info/news/ energy-efficiency-first-accelerating-towards-2030-objective-2019-sep-25 _ en. (accessed December 4, 2021)

European Commission, Energy performance of buildings, Energy - Eur. Comm. (2014) https://ec.europa.eu/energy/en/topics/energy-efficiency/ energy- performance- of-buildings/overview. (accessed December 4, 2021)

Fumo, M., Formisano, A., Sibilio, G., Violano, A. (2018). Energy and seismic recovering of ancient hamlets: The case of Baia e Latina. Sustainability, 10(8), 2831.

Furtado, A., de Risi, M.T. (2020). Recent findings and open issues concerning the seismic behaviour of masonry infill walls in RC buildings. Advances in Civil Engineering, 2020.

Garay, R., Arregi, B., Elguezabal, P. (2017). Experimental thermal performance assessment of a prefabricated external insulation system for building retrofitting. Procedia environmental sciences, 38, 155-161.

Ha, S. K., Yu, S. Y., Kim, J. S. (2018). Experimental study on existing reinforced concrete frames strengthened by L-type precast concrete wall panels to earthquake-proof buildings. KSCE Journal of Civil Engineering, 22(9), 3579-3591.

Iervolino, I., Galasso, C., Cosenza, E. (2010). REXEL: computer aided record selection for code-based seismic structural analysis. Bulletin of Earthquake Engineering, 8(2), 339-362.

ISTAT (2011). 15° Censimento generale della popolazione e delle abitazioni. https://www.istat.it/ (in Italian)

Ju, R. S., Lee, H. J., Chen, C. C., Tao, C. C. (2012). Experimental study on separating reinforced concrete infill walls from steel moment frames. Journal of Constructional Steel Research, 71, 119-128.

Kaushik, H. B., Rai, D. C., Jain, S. K. (2007). Stress-strain characteristics of clay brick masonry under uniaxial compression. Journal of materials in Civil Engineering, 19(9), 728-739.

Kaya, F., Tekeli, H., Anil, Ö. (2018). Experimental behavior of strengthening of masonry infilled reinforced concrete frames by adding rebar- reinforced stucco. Structural Concrete, 19(6), 1792-1805.

Konstantinou, T., Guerra-Santin, O., Azcarate-Aguerre, J., Klein, T., Silvester, S. (2017, January). A zero-energy refurbishment solution for residential apartment buildings by applying an integrated, prefabricated façade module. In Proceedings of the PowerSkin Conference, Munich, Germany (pp. 231-240).

Koutas, L., Pitytzogia, A., Triantafillou, T. C., Bousias, S. N. (2014). Strengthening of infilled reinforced concrete frames with TRM: Study on the development and testing of textile-based anchors. Journal of Composites for Construction, 18(3), A4013015.

Kyriakides, M. A., Billington, S. L. (2014). Cyclic response of nonductile reinforced concrete frames with unreinforced masonry infills retrofitted with engineered cementitious composites. Journal of Structural Engineering, 140(2), 04013046.

Lin, K., Totoev, Y. Z., Liu, H., Guo, T. (2016). In-plane behaviour of a reinforcement concrete frame with a dry stack masonry panel. Materials, 9(2), 108.

Mander, J. B., Priestley, M. J., Park, R. (1988). Theoretical stress-strain model for confined concrete. Journal of structural engineering, 114(8), 1804-1826.

Manfredi, V., Masi, A. (2018). Seismic strengthening and energy efficiency: Towards an integrated approach for the rehabilitation of existing RC buildings. Buildings, 8(3), 36.

Marini, A., Passoni, C., Belleri, A., Feroldi, F., Preti, M., Metelli, G., Plizzari, G. (2017). Combining seismic retrofit with energy refurbishment for the sustainable renovation of RC buildings: A proof of concept. European Journal of Environmental and Civil Engineering, 1-21.

Martiradonna, S., Fatiguso, F., Lombillo, I. (2020, June). Thermal improvements of existing reinforced concrete buildings by an Innovative Precast Concrete Panel system. In Colloqui. AT. e 2020, New horizons for sustainable architecture.

Masera, G., Seghezzi, E. (2015). Building retrofit through prefabricated panels: an overview on the state of the art. In 3rd International Congress on Construction and Building Research-COINVEDI (pp. 241-242). Escuela Técnica Superior de Edificación, Universidad Politécnica de Madrid.

Martiradonna S., INTELLIGENT PRECAST CONSTRUCTION SYSTEMS: Project, realization, maintenance technology for the optimization of the environment and economic sustainability (2021), PhD Thesis.

Miloni R., Grischott N., Zimmermann M. (2011). Building Renovation Case Studies (IEA ECBCS No. Annex 50), Switzerland: IEA. (accessed December 4, 2021)

Mondal, G., Jain, S. K. (2008). Lateral stiffness of masonry infilled reinforced concrete (RC) frames with central opening. Earthquake spectra, 24(3), 701-723.

Morandi, P., Milanesi, R. R., Magenes, G. (2018). Innovative solution for seismic-resistant masonry infills with sliding joints: in-plane experimental performance. Engineering Structures, 176, 719-733.

Negro, P., Colombo, A. (1997). Irregularities induced by nonstructural masonry panels in framed buildings. Engineering Structures, 19(7), 576-585.

Ozturkoglu, O., Ucar, T., Yesilce, Y. (2017). Effect of masonry infill walls with openings on nonlinear response of reinforced concrete frames. Earthquakes and Structures, 12(3), 333-347.

Panagiotakos TB, Fardis MN. (1996) Seismic response of infilled RC frames structures. In: Proceedings of 11th world conference on earthquake engineering. Acapulco [Paper No. 225].

Pasca, M., Liberatore, L. (2015). Predicting models for the evaluation of out-of-plane ultimate load carrying capacity of masonry infill walls. WIT Transactions on the Built Environment, 152, 83-94.

Pihelo, P., Kalamees, T., Kuusk, K. (2017). nZEB renovation with prefabricated modular panels. Energy Procedia, 132, 1006-1011.

Pittau, F., Malighetti, L. E., Iannaccone, G., Masera, G. (2017). Prefabrication as large-scale efficient strategy for the energy retrofit of the housing stock: An Italian case study. Procedia Engineering, 180, 1160-1169.

Pohoryles, D. A., Maduta, C., Bournas, D. A., Kouris, L. A. (2020). Energy performance of existing residential buildings in Europe: A novel approach combining energy with seismic retrofitting. Energy and Buildings, 223, 110024.

Porco, F., Fiore, A., Uva, G., Raffaele, D. (2015). The influence of infilled panels in retrofitting interventions of existing reinforced concrete buildings: A case study. Structure and Infrastructure Engineering, 11(2), 162-175.

Preti, M., Bettini, N., Plizzari, G. (2012). Infill walls with sliding joints to limit infill-frame seismic interaction: large-scale experimental test. Journal of Earthquake Engineering, 16(1), 125-141.

Ricci, P., Di Domenico, M., Verderame, G. M. (2018). Empirical- based out- of- plane URM infill wall model accounting for the interaction with in- plane demand. Earthquake Engineering & Structural Dynamics, 47(3), 802-827.

Ruggieri, S., Porco, F., Uva, G., Vamvatsikos, D. (2021). Two frugal options to assess class fragility and seismic safety for low-rise reinforced concrete school buildings in Southern Italy. Bulletin of Earthquake Engineering, 19(3), 1415-1439.

Ruggieri, S., Uva, G. (2020). Accounting for the spatial variability of seismic motion in the pushover analysis of regular and irregular rc buildings in the new Italian building code. Buildings, 10(10), 177.

Shing, P. B., Mehrabi, A. B. (2002). Behaviour and analysis of masonry- infilled frames. Progress in Structural Engineering and Materials, 4(3), 320-331.

Silva, P. C., Almeida, M., Bragança, L., Mesquita, V. (2013). Development of prefabricated retrofit module towards nearly zero energy buildings. Energy and Buildings, 56, 115-125.

The European Commission, Recomendations on building renovation, Official Journal of the European Union (2019). 6(L127/34), pp. 34–79. https://eur-lex.europa.eu/legal-content/EN/TXT/?qid=1442476465850&uri=CELEX:32019H0786.

Tsantilis, A. V., Triantafillou, T. C. (2018). Innovative seismic isolation of masonry infills using cellular materials at the interface with the surrounding RC frames. Engineering Structures, 155, 279-297.

Ursini Casalena, A. (2018) Trasmittanza Termica Periodica: Foglio di Calcolo Excel UNI 13786 per Calcolare le Proprietà Termiche Dinamiche di un Componente Edilizio, www.mygreenbuildings.org. (Accessed: 29 November 2020).

Uva, G., Raffaele, D., Porco, F., Fiore, A. (2012). On the role of equivalent strut models in the seismic assessment of infilled RC buildings. Engineering Structures, 42, 83-94.

Valluzzi, M. R., Da Porto, F., Garbin, E., Panizza, M. (2014). Out-of-plane behaviour of infill masonry panels strengthened with composite materials. Materials and structures, 47(12), 2131-2145.